NOTICE

CERTAIN DATA CONTAINED IN THIS DOCUMENT MAY BE DIFFICULT TO READ IN MICROFICHE PRODUCTS.

SAND--90-0485

DE91 000457

SAND90-0485
Unlimited Release
Printed August 1990

Ground Shock from Multiple Earth Penetrator Bursts: Effects for Hexagonal Weapon Arrays

L.N.Kmetyk
Computational Physics & Mechanics Division I
P.Yarrington
Computational Physics & Mechanics Division II
Sandia National Laboratories
Albuquerque, New Mexico 87185

Abstract

Calculations have been performed with the HULL hydrocode to study ground shock effects for multiple earth penetrator weapon (EPW) bursts in hexagonal-close-packed (HCP) arrays. Several different calculational approaches were used to treat this problem. The first simulations involved two-dimensional (2D) calculations, where the hexagonal cross-section of a unit-cell in an effectively-infinite HCP array was approximated by an inscribed cylinder. Those calculations showed substantial ground shock enhancement below the center of the array. To refine the analysis, 3D unit-cell calculations were done where the actual hexagonal cross-section of the HCP array was modelled. Results of those calculations also suggested that the multiburst array would enhance ground shock effects over those for a single burst of comparable yield. Finally, 3D calculations were run in which an HCP array of seven bursts was modelled explicitly. In addition, the effects of non-simultaneity were investigated. Results of the seven-burst HCP array calculations were consistent with the unit-cell results and, in addition, provided information on the 3D lethal contour produced by such an array.

Contents

Tables

Figures

1. Introduction

A spaced array of subsurface bursts detonated simultaneously would be expected to result in significantly enhanced ground shock effects when compared to an equal number of identical bursts detonated independently, *i.e.*, with a sufficiently long time delay between bursts that no ground shock interactions would occur. The simultaneous multiburst array will direct ground shock energy perpendicular to the array plane (*i.e.*, upward and downward). In fact, directly below the center of the array, an optimized multiburst scheme would be expected to produce higher levels of stress than a single burst of the same total yield, or same *aggregated yield*, as that of the array.

This report presents results of two-dimensional (2D) and three-dimensional (3D) HULL [1] hydrocode calculations of ground shock from simultaneous detonations of multiple earth penetrator weapons (EPWs). The EPWs were assumed to be arranged in an hexagonal-close-packed (HCP) array, as shown in Figure 1.1. Each burst in the array was assumed to have a nominal yield of 500kt and a depth-of-burst (DOB) of 12m, and the target material was modelled as a homogeneous, wet, soft rock. The baseline weapon spacing was taken to be 400m, but various other spacings were considered in sensitivity studies.

The yield of 500kt was chosen for the present studies as a nominal yield representative of fieldable EPW technology, while recognizing that lower yield weapons would probably be more realistic for a multiburst targeting scheme. Of course, as will be demonstrated later in the report, it is possible to use scaling arguments to generalize these results to arrays involving weapons of somewhat smaller yield. The seven burst hexagonal array modeled here probably also represents a bounding case, in terms of the number of weapons that would be targeted on any site. Two or three weapons would, in fact, be a more likely deployment. The HCP array was chosen, however, because it has the advantage of being representable, to a good first approximation, as a cylindrically-symmetric problem for analyses of ground shock effects. Thus, two-dimensional hydrocode calculations could be used to model this problem and, thereby, explore relatively inexpensively the ground shock enhancement from a multiburst targeting scheme.

Calculations are presented which simulate ground shock effects for: 1) an array involving a large number of weapons, *i.e.*, an "effectively" *infinite* array, and 2) a *finite* array involving seven bursts. Details on the source and target modelling are provided in Section 2, while descriptions of the computational models used for the various calculations discussed in this report are given in Appendix A.

For an "effectively" *infinite* HCP array (*i.e.*, one involving a relatively large number of bursts), the problem has symmetry planes as shown in Figure 1.2 and can be simulated

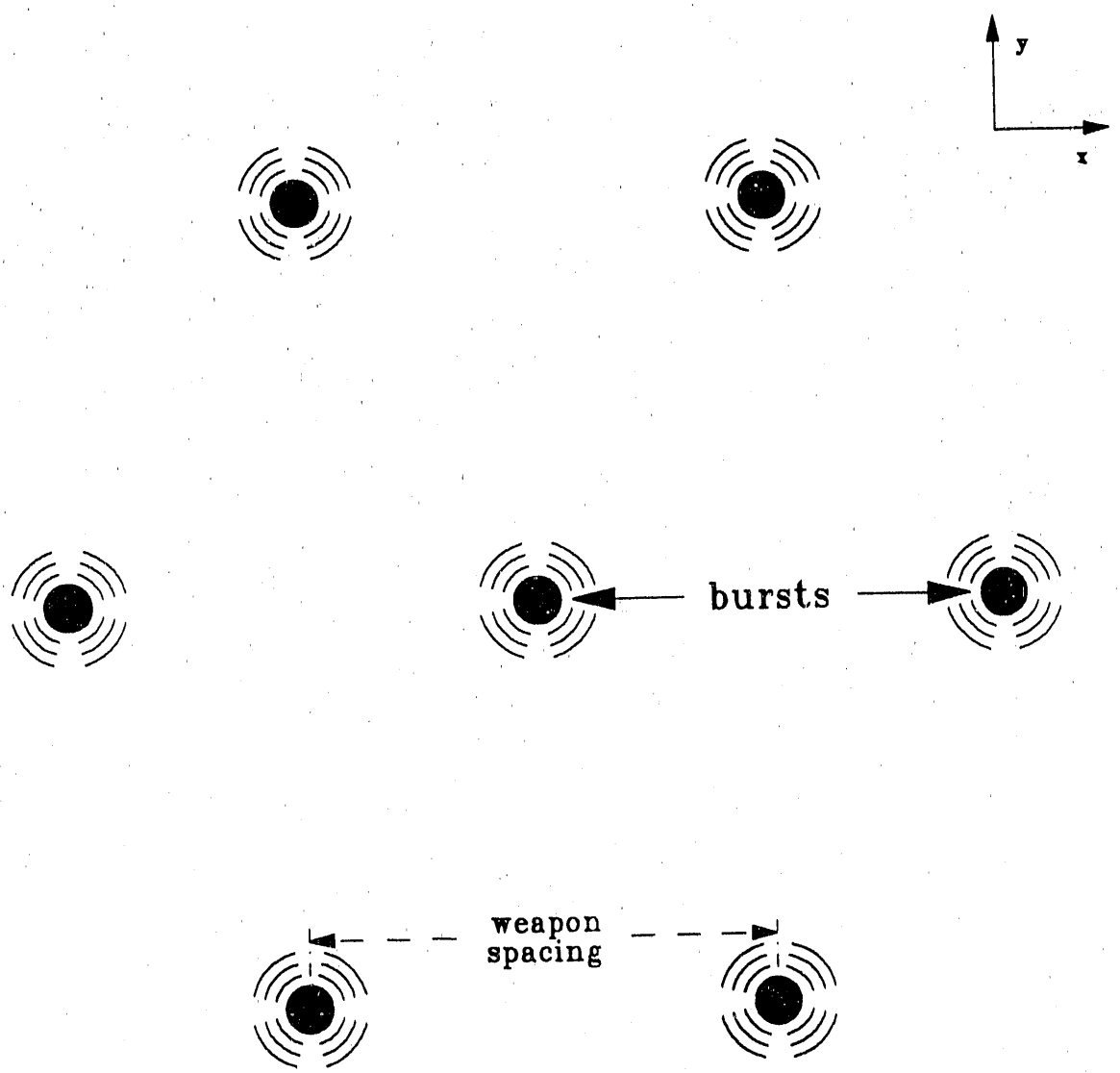

Figure 1.1. Hexagonal-Close-Packed (HCP) Multiburst Array Geometry

by analysis of ground shock effects for the "unit-cell" of hexagonal cross-section shown in the figure. As will be demonstrated below, this simulation also provides a good approximation to the ground shock effects below the central burst in a *finite* HCP array (*e.g.*, a seven-burst array), at least to moderate depths (*i.e.*, comparable to the weapon spacing in the array) below the ground surface. Furthermore, the geometry of the hexagonal-unit-cell problem suggests the use of a circular-unit-cell, inscribed in the hexagonal cell as shown in Figure 1.3, to *approximate* the ground shock effects from the array. This then results in a simpler, two-dimensional, cylindrically-symmetric model for the problem, which will give an "upperbound" estimate of the ground shock stress levels below the array.

Section 3 presents results of such 2D circular-unit-cell calculations, showing ground shock effects for EPW multiburst arrays with various burst spacings. To complete the "unit-cell" studies, Section 4 presents results of 3D calculations which model the actual hexagonal geometry for a unit-cell in the HCP array. Comparisons are shown between the 2D and 3D unit-cell calculations, and results of parameter studies on weapon spacing are also presented.

The unit-cell calculations provide useful estimates of the *maximum* depth in the target to which a particular level of ground shock would be delivered by the multiburst array. However, these calculations are limited in terms of predicting ground shock lethal effects from a multiburst array. In particular, the unit-cell calculations simulate effects for an *infinite* array, thus attenuation of the waves due to lateral dispersion beyond the edge of the array is not treated with this approach. Therefore, they give no information on the lateral (horizontal) extent of the lethal ground shock contour, *i.e.*, the lethal "footprint", that would be expected from a *finite* multiburst array. To complete the present study, 3D calculations were performed which modelled a *finite*, seven-burst, HCP array. Results of those calculations are presented in Section 5, along with comparisons between the finite array results and the unit-cell calculations.

Section 6 provides a summary of the study. Input listings and code changes used for the calculations are given in Appendix B, along with file storage information, for reference.

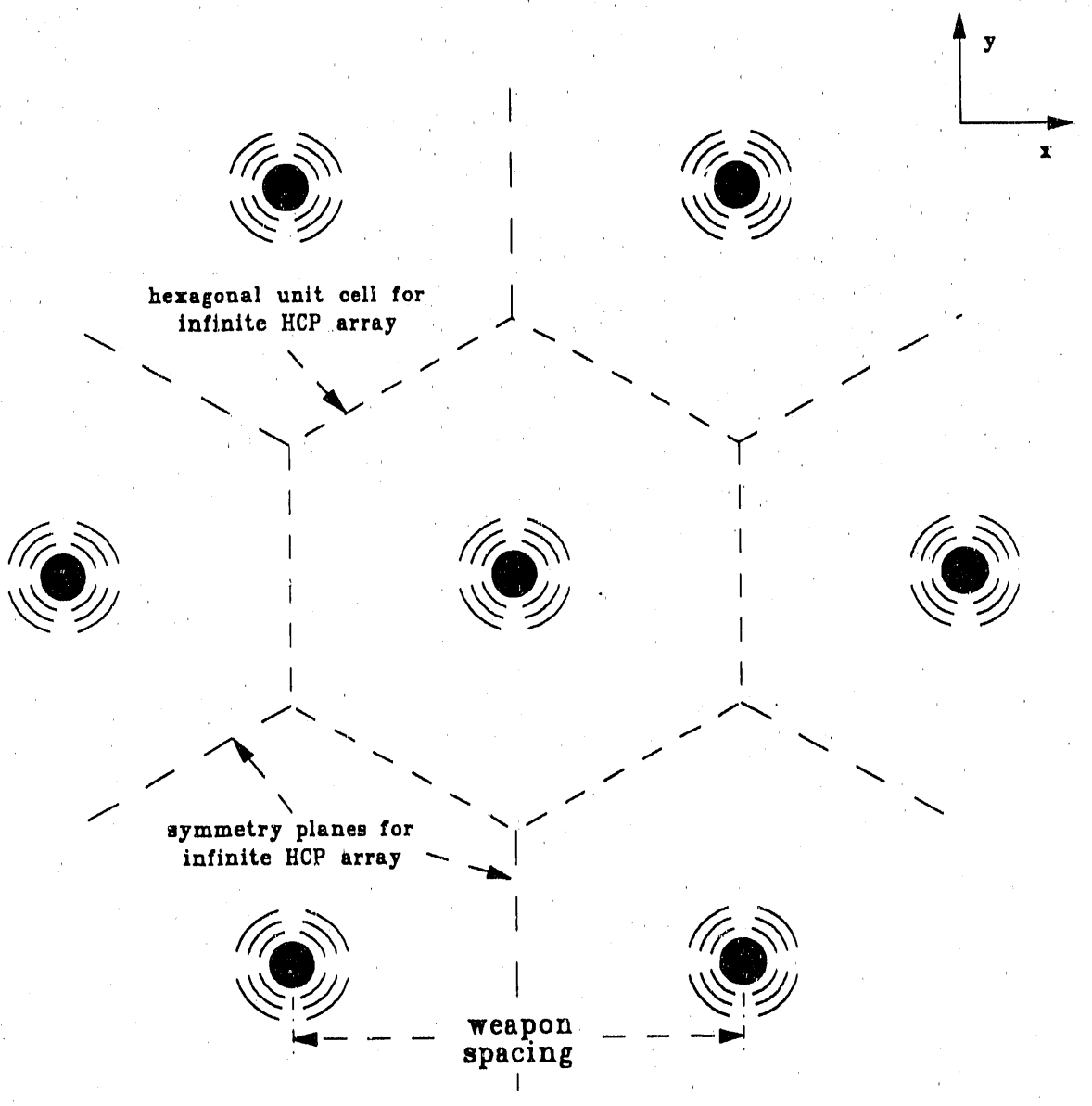

Figure 1.2. Symmetry Boundaries and Hexagonal-Unit-Cell for "Infinite" HCP Array

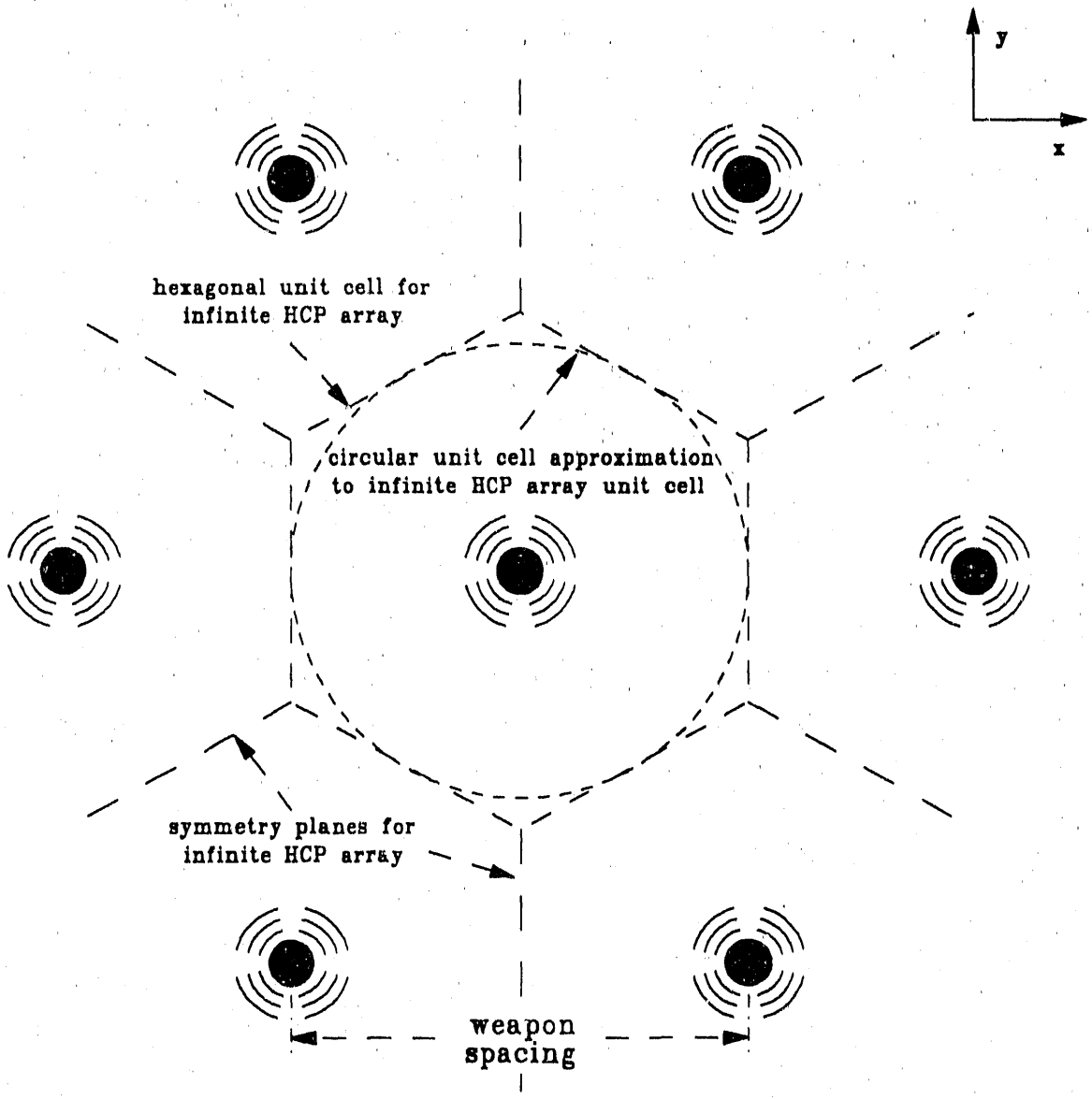

Figure 1.3. Circular-Unit-Cell Approximation for HCP Array

2. Problem Description

The HULL code system [1] consists of a set of computer programs for generating and solving continuum dynamics problems, plus assorted peripheral programs such as are required, for example, to produce plots. As currently configured, HULL can solve two- and three-dimensional Eulerian and Lagrangian problems, and provides various means for linking these two types of solutions. For the present study, all calculations were run in the Eulerian mode.

The energy release of the EPW bursts was modelled in the calculations by instantaneously depositing the yield of the weapon (*i.e.*, 500kt) in a 1m-radius sphere of the geologic target material centered at the 12m DOB. The target material was assumed to be uniform and undisturbed in all directions surrounding the burst location. For deeply-buried bursts such as those considered here, energy transfer by radiation transport is insignificant and was not included in the calculations.

Virtually all material property data (except air) are read from an extensive material library file (MATLIB). This file includes both the equation-of-state (EOS) of the material and its strength properties. The user can change the basic data for a material or add new materials, as long as they can be represented by one of the EOS types in MATLIB. The ground material for this work was modelled with the Mie-Gruneisen EOS available in the code, and Table 2.1 lists the material constants that were used. Material strength effects were ignored in these calculations.

In the various unit-cell calculations that were done for this study, symmetry planes that did not lie along one of the coordinate planes were treated with the HULL "island" option. This option allows regions of the calculational grid to be treated as rigid bodies. The boundaries of such regions are, therefore, "perfectly" reflective and equivalent to symmetry boundaries for the problem. It should be noted that the boundary of a HULL island region follows the grid lines of the calculational mesh and will, therefore, represent smooth surfaces in a "stairstep" fashion. This is illustrated in Section 2 of Appendix A for the hexagonal-unit-cell calculations.

The automatic rezoning logic in the HULL program was substantially modified for the present calculations, in large part to ensure that both two- and three-dimensional analyses used exactly the same mass-, momentum- and internal-energy-conserving, rezone scheme. These modifications are discussed in more detail in the input model descriptions of Appendix A. A listing of the rezone change deck used for the present calculations is included in Appendix B, for reference.

```
material property data for material named air
                ambient density =  1.2250e-03
          ambient sound speed =  3.4029e+04
               ambient energy =  2.0679e+09
                        gamma =  1.4000e+00
units are assumed to be cgs

material property data for material named mtuff
                ambient density =  2.0000e+00
          ambient sound speed =  2.8000e+05
shock vel/particle vel slope =  1.0100e+00
               gruneisen ratio =  1.0000e+00
             minimum pressure = -1.0000e+08
               poissons ratio =  2.5000e-01
             rigidity modulus =  9.4080e+10
                atomic weight =  0.6000e+02
            debye temperature =  0.3800e+03
      vapor state coefficient =  0.2500e+00
                ambient energy =  0.6798e+09
          ambient melt energy =  0.1000e+11
                fusion energy =  0.8000e+10
           sublimation energy =  0.1200e+12
energy at beginning of vapor =  0.5000e+11
        energy at end of vapor =  0.1000e+12
        initial yield strength =  1.0000e+09
        maximum yield strength =  1.0000e+09
      strain at maximum yield =  3.0000e-01
thermal softening coeff   yf1 =  9.0000e-01
thermal softening coeff   ef1 =  9.0000e-01
thermal softening coeff   yf2 =  9.0000e-01
thermal softening coeff   ef2 =  9.0000e-01
  principal stress at failure =  0.1000e+21
  principal strain at failure =  0.1000e+21

 units are assumed to be cgs
```

Table 2.1. HULL Material Property Data

3. Circular-Unit-Cell Calculations

For the case in which there is a relatively large number of weapons in an HCP array, the multiburst problem can be simulated by analysis of effects in a unit-cell of hexagonal cross-section, as was shown in Figure 1.2. The geometry of this problem then suggests the use of a simplified, two-dimensional, cylindrically-symmetric approximation, as is illustrated in Figure 1.3, to calculate ground shock effects for the array. This section of the report presents results of a series of such 2D calculations that was performed to estimate ground shock effects from multiburst arrays for various burst spacings and depths. The HULL input model for these 2D analyses is described in detail in Appendix A.1.

3.1 Baseline Study

Figure 3.1 shows the pressure profiles on axis and pressure contours at a problem time of 25ms for a single 500kt burst at 12m DOB. The shock front has reached a radius of ~150m at this time. For an HCP array of such bursts spaced 400m apart and detonated simultaneously, this result clearly represents each of the separate bursts in the array at that time, since no interactions between the bursts could yet have occurred. The expanding ground shock front reaches 200m in radius at ~50ms and, thus, encounters the unit-cell boundary, as shown in the first plot of Figure 3.2. In the present 2D approximation, reflection from the unit-cell boundary represents interaction with the shock waves from the surrounding bursts in the array. The pressure contour plots of Figure 3.2 show how the reflected, reinforced shock reconverges below the burst in the 100-200ms time interval and delivers a strong second pulse to points deep in the target. Due to wave interactions with the transient crater, and to other free surface effects, the reflected shock reconverges on axis at some considerable depth (~200-250m) below the original burst position. Notice in Figure 3.2 that the shock front becomes relatively planar in shape as time progresses.

3.2 Single Burst versus Multiburst Comparison

Figure 3.3 shows a comparison of peak pressure versus depth below ground surface for:

1. a single 500kt burst,
2. a single "equivalent" 3.5Mt burst (*i.e.*, a single burst of the same *aggregated yield* as seven 500kt bursts in an HCP array),

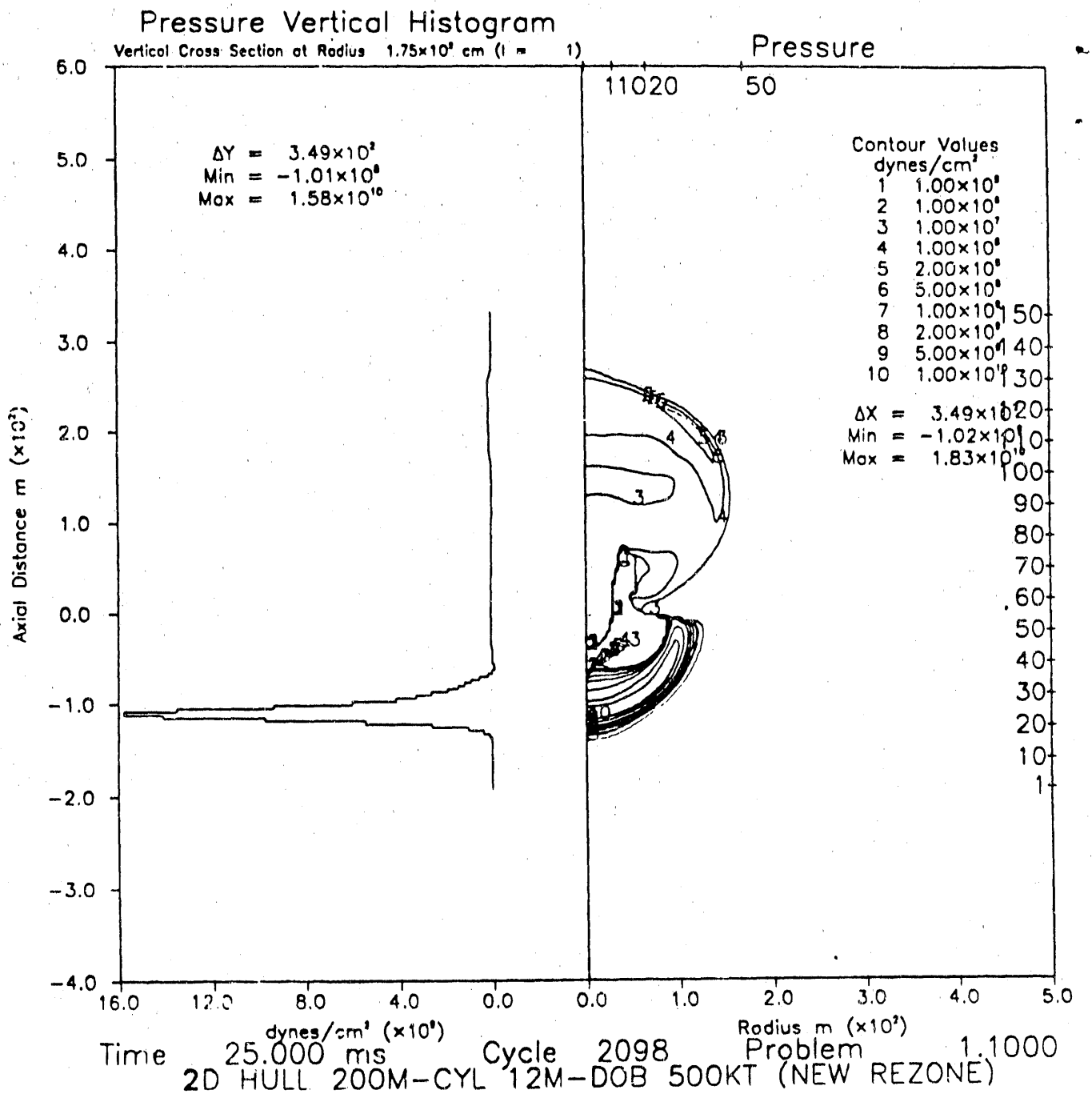

Figure 3.1. Pressure Profiles on Axis and Pressure Contours for Circular-Unit-Cell Calculations at Problem Time of 25ms)

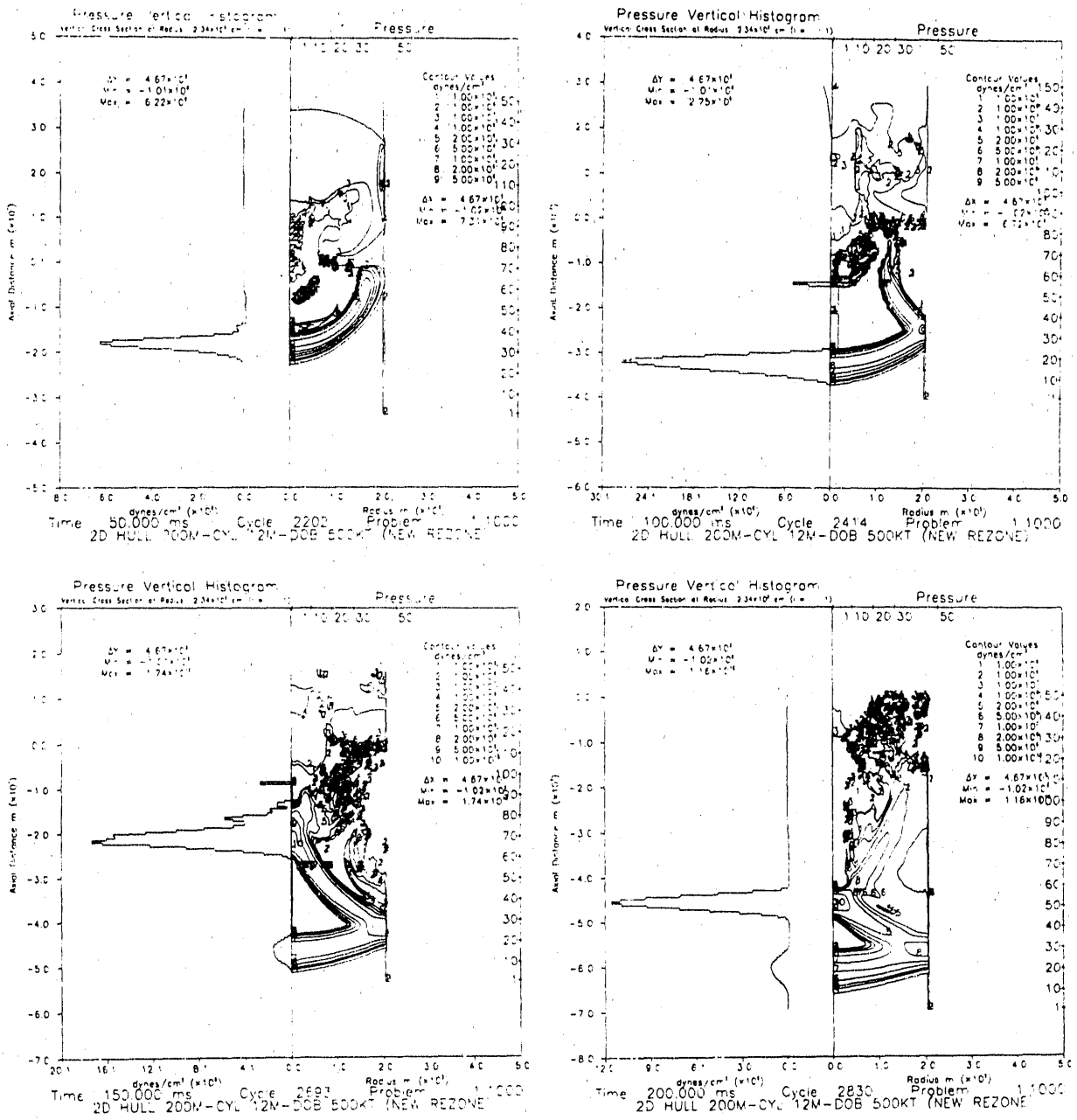

Figure 3.2. Pressure Profiles on Axis and Pressure Contours for Circular-Unit-Cell Calculations at Problem Times of 50ms (top left), 100ms (top right), 150ms (bottom left), and 200ms (bottom right)

3. a single 20Mt burst (obtained by cube-root-scaling of the 3.5Mt single burst results), and

4. the 2D unit-cell calculation, simulating an HCP array of 500kt bursts with 400m burst separation.

All results in Figure 3.3 were obtained from 2D HULL calculations for bursts at 12m DOB, with the exception of the 20Mt burst which was scaled from results for the 3.5Mt single burst. The pressure delivered by a single burst attenuates monotonically with distance as the pulse propagates radially outward and downward. In a multiburst array, however, the initial shock delivered to points on axis below any of the bursts is followed, and overtaken, by a second wave due to interaction and convergence of the shock fronts from the surrounding bursts. This enhancement of ground shock effects from wave interactions in the multiburst array can be clearly seen in the plot. Notice, again, that the reflected wave converges on axis at some depth below the original burst, due to wave interactions with the free surface and the edge of the transient crater.

In order to get the best estimate of effects for a seven burst array from the present circular-unit-cell calculations, care was taken in extracting the peak pressure results, shown in Figure 3.3, to get only effects of the *first* wave reflections from the cell boundary. With this approach, the results shown for the unit-cell calculation can be interpreted as a reasonable (though *upperbound*) estimate of the peak pressure directly under the central burst in a *finite* HCP array. The peak pressure on axis for the multiburst array is seen to be enhanced by a factor of ~4-5 over the pressure delivered by a single 500kt burst, and enhanced by a factor of ~2-3 over the pressure delivered by a single 3.5Mt burst. Similarly, in terms of depth-to-effect, the array delivers a given pressure level to significantly greater depths. For example, while single 500kt and 3.5 Mt bursts deliver a peak pressure of 0.5kb to depths of ~900m and ~1750m, respectively, the 2D unit-cell calculations suggest that an HCP multiburst array representing a 3.5Mt *aggregated* yield delivers a peak pressure of 0.5kb to a depth of ~2250m. This can be seen to be roughly equivalent to the ground shock effects from a 20Mt EPW burst.

3.3 Sensitivity Studies

Spacing Study

Additional 2D unit-cell calculations were done to investigate the influence of weapon spacing on predicted ground shock effects for the array. In particular, calculations were done to model weapon spacings of 100m, 200m, 400m and 800m. This was accomplished by setting the radius of the circular-unit-cell to 50, 100, 200, and 400m, respectively. An (x-y) grid of 50×150 zones was used for all calculations, and the ratio of overall x and y dimensions was held constant at 1:3, as in the baseline calculations. The initial cell size was 25cm in all cases. The automatic, expanding rezoner allowed the mesh (and cell size)

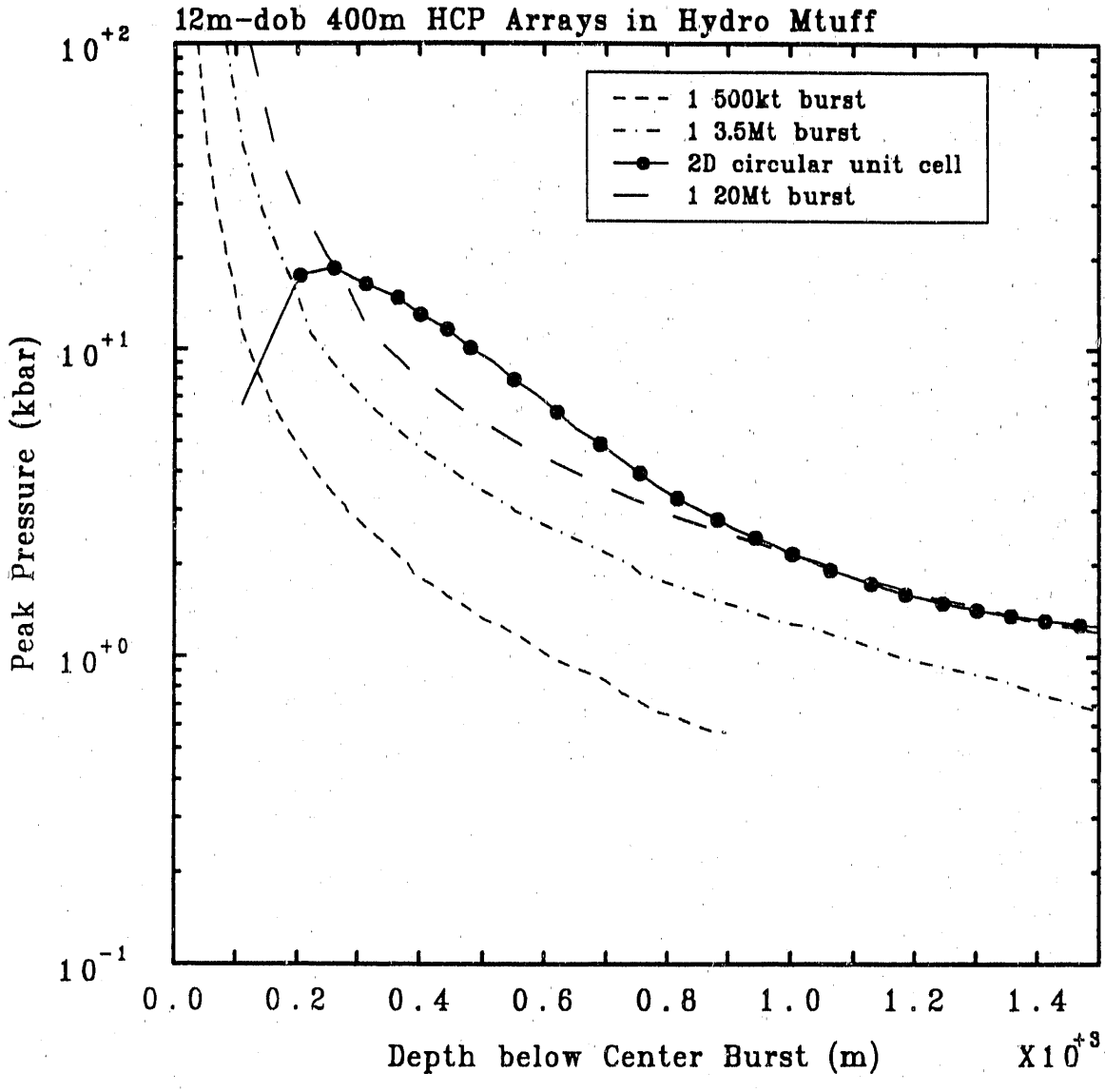

Figure 3.3. Peak Pressure versus Depth for Circular-Unit-Cell and Single Burst Calculations

to grow as required until the boundary of the unit-cell was reached, at which time the translating rezoner followed the wave as it propagated into the target. (Note that, with this approach, the zoning was different during late stages of the calculations for each of the burst spacings considered.)

The top plot in Figure 3.4 shows the predicted peak pressure versus depth for these four cases. It can be seen that the wave interactions occur at progressively higher pressure levels and shallower depths with reduced weapons spacings. Notice also that for the three smaller unit-cells (*i.e.*, the cases simulating arrays with smaller burst spacings) the results approach essentially the same attenuation curve after the early stages of wave interaction. (The reason why results for the 800m spacing remain somewhat below the other cases is not clear at this time.) The bottom plot in Figure 3.4 compares the results for the circular-unit-cell with those for single bursts of 500kt and 3.5Mt.

Zoning Study

Additional calculations were done to determine the sensitivity of the circular-unit-cell results to the zoning used for the problem. For this study, the problem of a 200m-radius circular-unit-cell was considered. For the finely-zoned calculation the number of zones was doubled, and for the coarsely-zoned calculation the number of zones was halved, in each direction, with respect to the baseline zoning of 50×150. The ratio of x and y overall dimensions was maintained constant at 1:3.

Figure 3.5 shows the predicted peak pressure versus depth for the three different zonings. It is clear that the calculation using the baseline zoning is not "fully-converged"; however, it was not practical in terms of computing time to run calculations in which the zoning was refined further. Thus, *assuming* that the finely-zoned calculation represents the "limiting" solution, calculations with the baseline zoning appear to be *underpredicting* (by $\sim$20%) the depth-to-effect, *i.e.*, the maximum depth to which a given peak pressure level is delivered. These results illustrate why care was taken to use similar zonings in the calculations compared in this study.

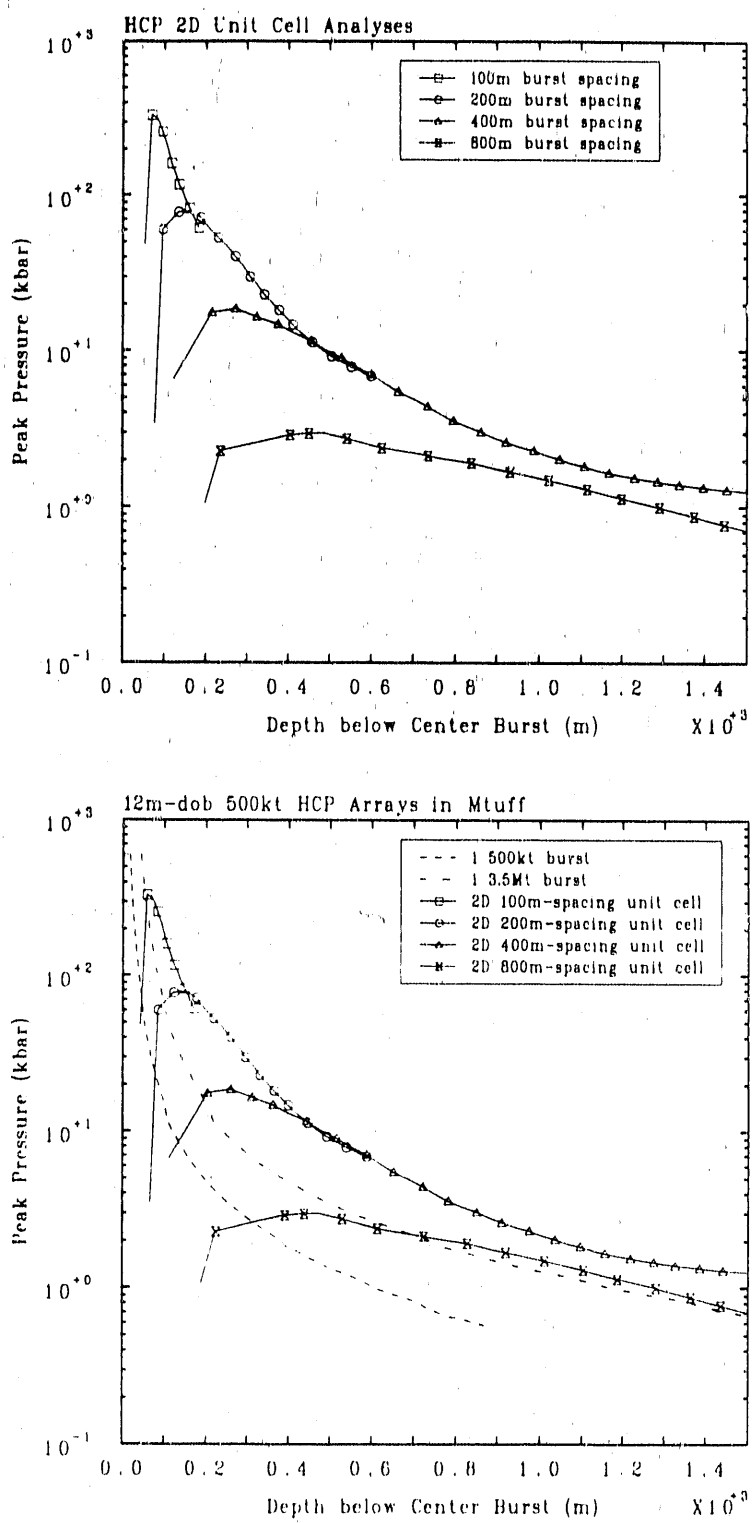

Figure 3.4. **Peak Pressure versus Depth for Circular-Unit-Cell Calculations Representing Different Weapon Spacings (top) and with Comparisons to Single Burst Results (bottom)**

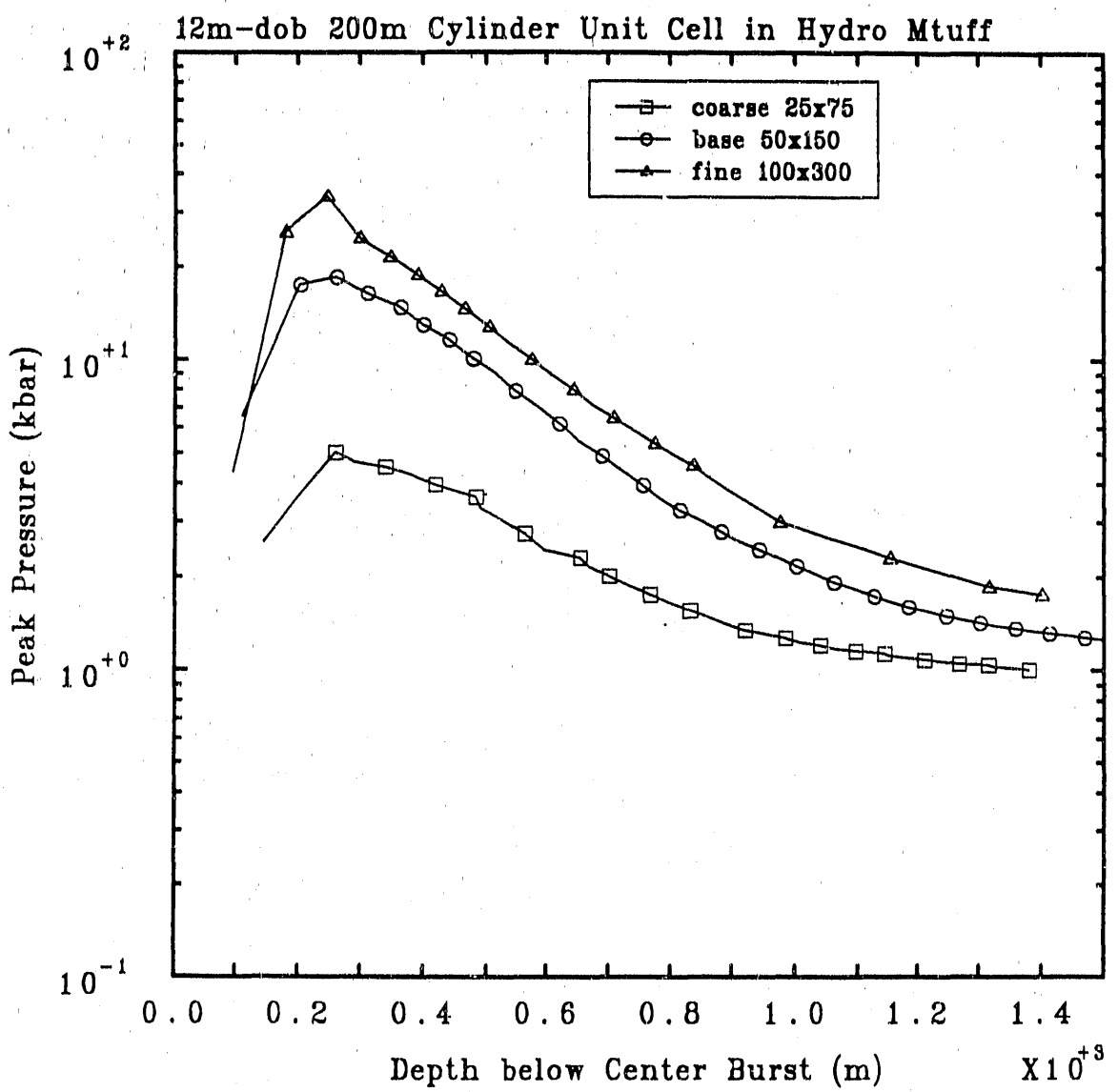

Figure 3.5. Peak Pressure versus Depth for Circular-Unit-Cell Zoning Study Calculations

4. Hexagonal-Unit-Cell Calculations

The results in the previous section were from two-dimensional calculations in which the hexagonal-unit-cell boundary of an *infinite* HCP array was approximated by an "equivalent" inscribed cylinder. To refine this analysis, three-dimensional calculations were performed in which the actual hexagonal-unit-cell geometry (see Figure 1.2) for such an array was modelled. A detailed description of the HULL input model is given in Appendix A.2. Note that, due to the symmetry of the problem, it was only necessary to model one quadrant of the unit-cell, as shown in Figure A.4.

4.1 Baseline Study

Figure 4.1 is a split-frame plot showing pressure contours on the x-z and y-z planes (left- and right-frames, respectively) at a sequence of times (viz., 50ms, 100ms, 150ms, and 200ms) for the baseline hexagonal-unit-cell calculation. At ~50ms, reflection from nearest portions of the unit-cell boundary is seen to occur, corresponding to the initial interaction of ground shock fronts from adjacent bursts in the HCP array. The reflected wavefronts sweep through the target behind the leading shock front and focus on axis to produce a strong, second pressure pulse. The flattening of the shock front due to wave interactions between bursts, as simulated by reflections from the unit-cell boundary, can also be seen in these results. Figure 4.2 shows a similar sequence of pressure plots, where the pressure profile on axis is shown in the left frame. The second pressure pulse which occurs behind the leading wave from the reflected shocks can be clearly seen in the later-time (*i.e.*, 150ms and 200ms) results.

4.2 Single Burst versus Multiburst Comparisons

Hexagonal-Unit-Cell versus Single Bursts

A comparison of peak pressure versus depth is shown in Figure 4.3, for the following calculations:

1. a single 500kt burst,
2. a single 3.5Mt burst,
3. a single 20Mt burst (obtained by cube-root-scaling of the 3.5Mt single burst results), and

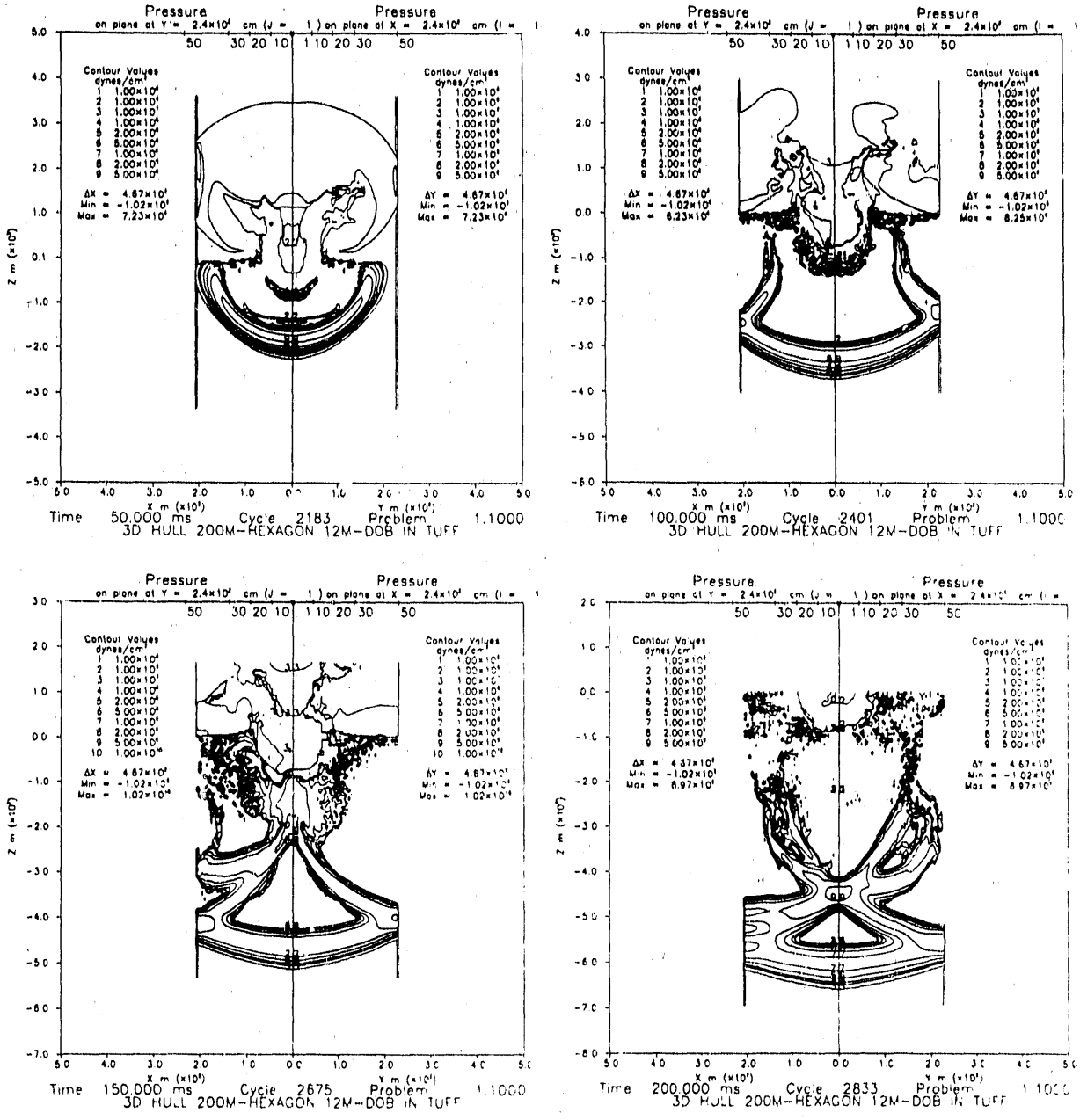

Figure 4.1. Pressure Contours (split-frame: (x-z) plane on left and (y-z) plane on right) for Hexagonal-Unit-Cell Calculations at Problem Times of 50ms (top left), 100ms (top right), 150ms (bottom left), and 200ms (bottom right)

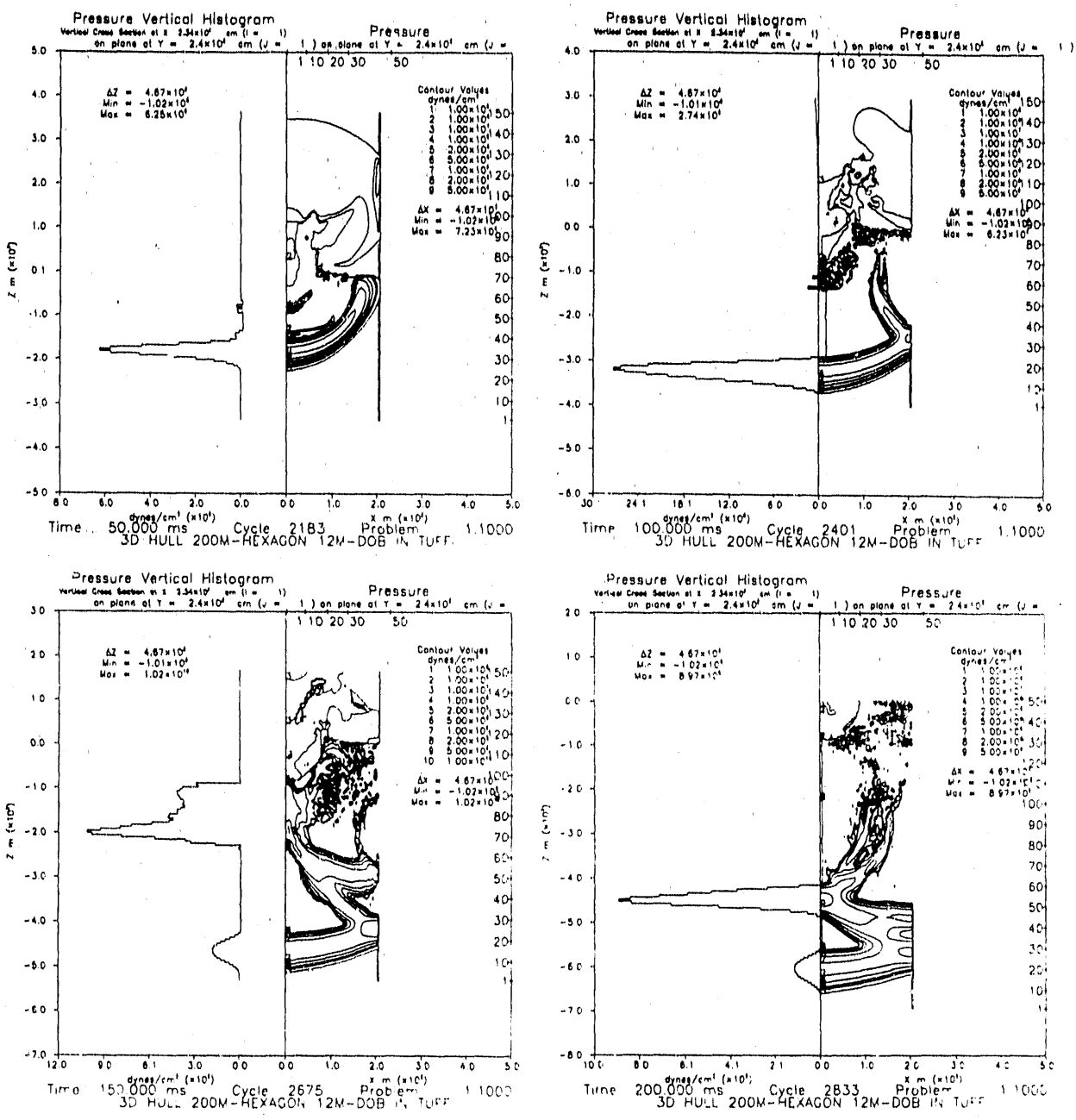

Figure 4.2. Pressure Profiles on Axis and Pressure Contours on (x-z) Plane for Hexagonal-Unit-Cell Calculations at Problem Times of 50ms (top left), 100ms (top right), 150ms (bottom left), and 200ms (bottom right)

4. the 3D hexagonal-unit-cell calculation, simulating an HCP array of 500kt bursts with 400m burst separation.

The peak pressure plotted in Figure 4.3 is for points directly under the burst, in both the single burst and the unit-cell "multiburst" calculations. By disregarding effects of late-time reflections from the unit-cell boundary, as discussed in Section 3.2, the peak pressure on axis in the unit-cell calculations is a reasonable (though, again, *upperbound*) estimate of effects below the central burst in a *finite*, seven-burst, HCP array. Thus, these results suggest that in terms of peak pressure on axis the HCP array is equivalent to a single burst of 20Mt, or about six times the *aggregated yield* of the seven-burst array.

Hexagonal-Unit-Cell (3D) versus Circular-Unit-Cell (2D)

The bottom plot in Figure 4.3 adds results of the circular-unit-cell (2D) calculations to the previous comparisons. Notice that the strength of the reflected wave for the circular-unit-cell is somewhat greater than that for the hexagonal-unit-cell at shallow depths, but becomes a very good approximation to the 3D results at greater depths, where pressure levels are in the kilobar range.

These results are as would be expected, since an *inscribed* circle was used in the 2D calculations to approximate the geometry of the hexagonal-unit-cell boundaries (see Figure 1.3). With this approach, all points on the reflecting boundary of the 2D circular-unit-cell are *equidistant* from the axis below the burst and as close to the axis as the *closest* points of the 3D hexagonal-unit-cell. Thus, the reflected waves in the 3D calculation must, in general, propagate further and will attenuate more by the time they return to the axis than in the 2D case. Furthermore, waves reflected from different points on the hexagonal-unit-cell boundary will not converge *coherently* on axis, as will be the case for the circular-unit-cell.

4.3 Sensitivity Studies

Spacing Study

Sensitivity of the multiburst effects to array spacing in the 3D unit-cell problems was investigated with additional calculations for weapon spacings of 100, 200, 400, and 800m, with the 400m spacing (*i.e.*, 200m unit-cell) identified as the *baseline* calculation. An (x-y-z) grid of 50×50×150 zones was used for all calculations, with the initial size of the cubical zones being 25cm. Expanding and translating rezone options, as discussed in Appendix A.2, were used to follow the ground shock outward and, ultimately, downward to the depths of interest in the target.

Figure 4.4 shows peak pressure versus depth obtained for these calculations, where the effect of array spacing can be seen to be quite similar to what was found in the 2D

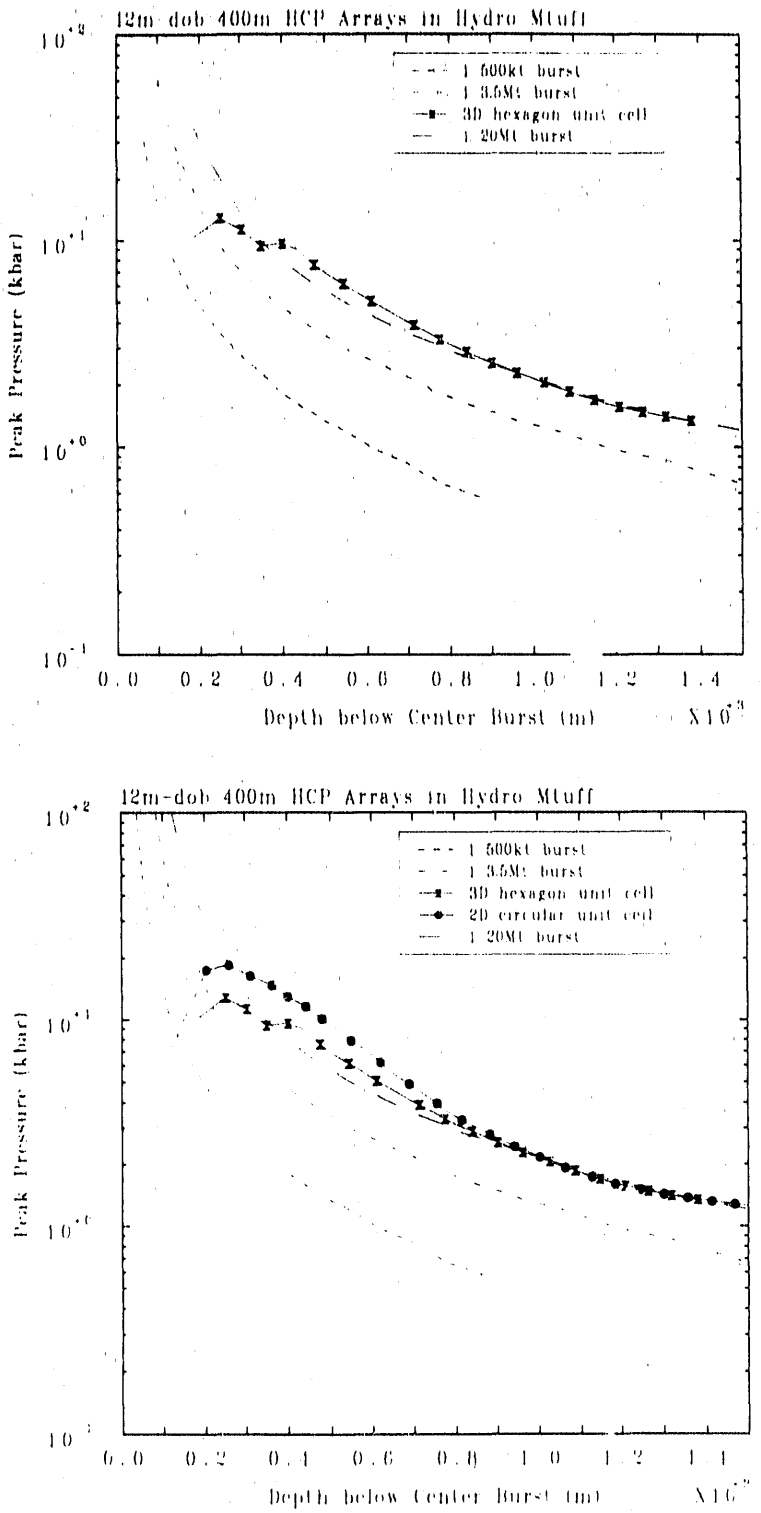

Figure 4.3. Peak Pressure versus Depth for Hexagonal-Unit-Cell Calculations Compared with Single Burst Results (top) and with Circular-Unit-Cell Results Added (bottom)

circular-unit-cell weapon spacing sensitivity study (see Fig. 3.4). In particular, we see that the results for the three smaller unit-cells approach the same attenuation curve after the early stages of wave interaction. The bottom plot in Figure 4.4 shows these results with the peak pressure curves for 500kt and 3.5Mt single bursts added to the figure.

The similarity in results for the 2D and 3D unit-cell weapon spacing studies is shown in Figure 4.5. Interestingly, the 2D results are seen to become a very good approximation to the results for the 3D geometry at depths about equal to the array spacing in each case.

Zoning Study

To determine the sensitivity of the results to the numerical resolution, the baseline problem was rerun with the zoning made coarser by a factor of two in each direction, *i.e.*, $25\times25\times75$ zones. The ratio of overall x, y and z dimensions was maintained constant at 1:1:3, with the cell size expanded as required to cover the same distance. The zoning is described in more detail in Appendix A.2. Note that *increasing* the resolution of the baseline mesh by a factor of two in each direction was considered impractical in three dimensions, due to both computer memory and calculational cost considerations.

Peak pressure versus depth, as predicted for the baseline and coarsely-zoned calculations, is shown in Figure 4.6. Similar effects were seen in the 2D unit-cell zoning sensitivity study discussed in Section 3.3, and the results of those calculations are added to the 3D results in the bottom plot of Figure 4.6. Thus, as in the 2D case (see Section 3.3), we conclude that the baseline calculations are showing the right qualitative trends, but are underpredicting the depth-to-effect by $\sim$20%.

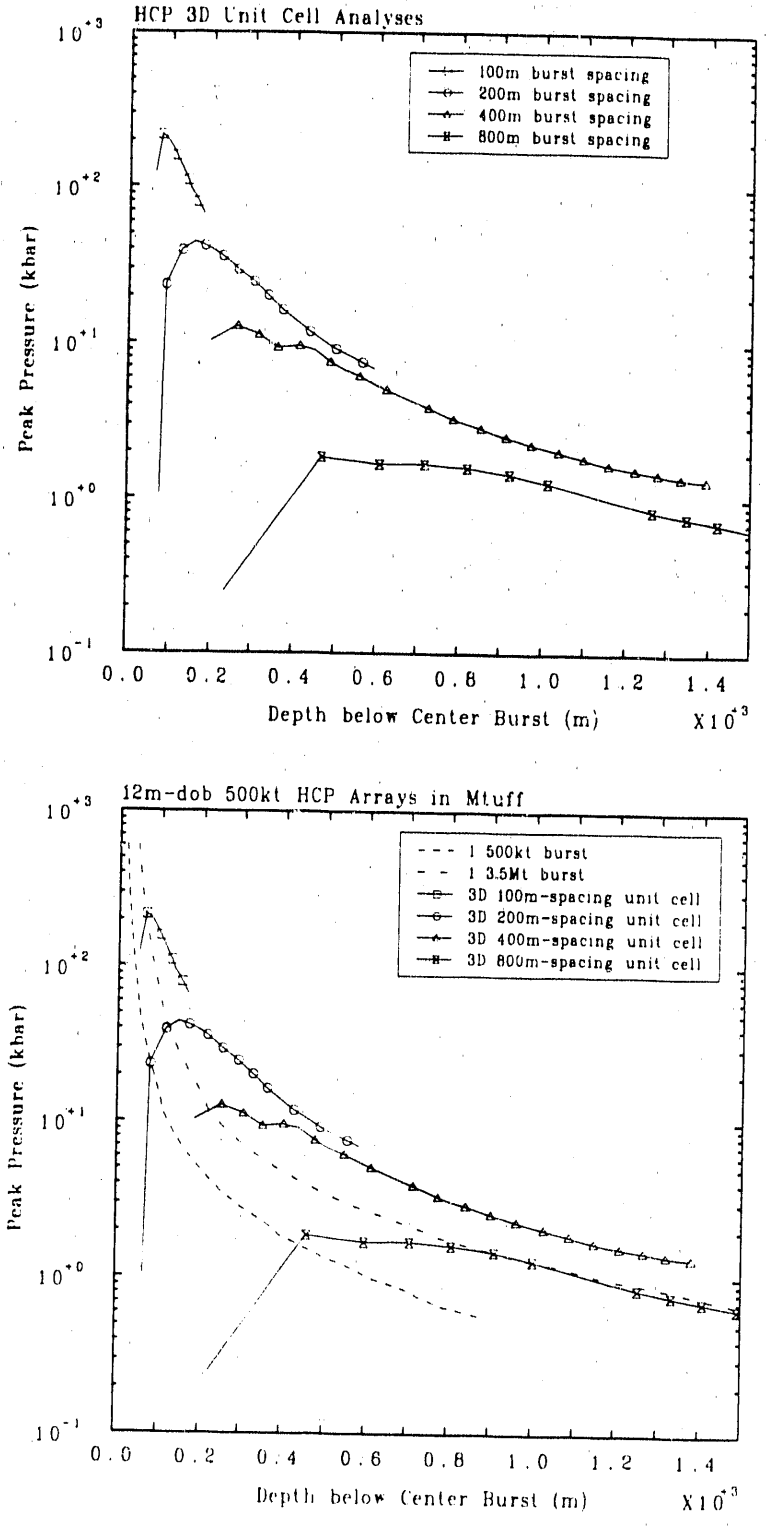

Figure 4.4. Peak Pressure versus Depth for Hexagonal-Unit-Cell Calculations Representing Different Weapon Spacings (top) and with Comparisons to Single Burst Results (bottom)

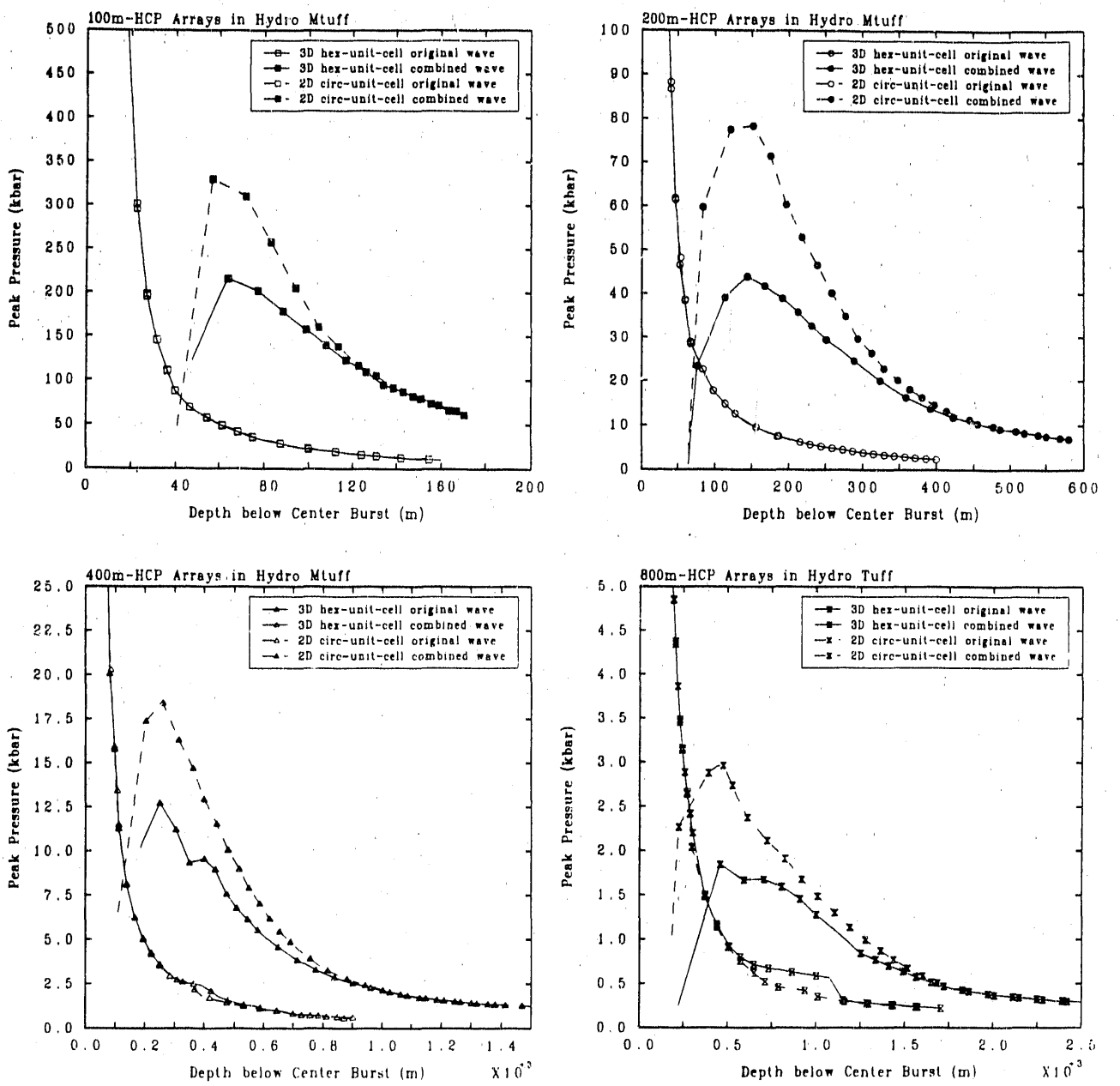

Figure 4.5. Peak Pressure versus Depth for Circular-Unit-Cell and Hexagonal-Unit-Cell Calculations with Weapon Spacing of 100m (top left), 200m (top right), 400m (bottom left), and 800m (bottom right); "Original Wave" represents single 500kt burst

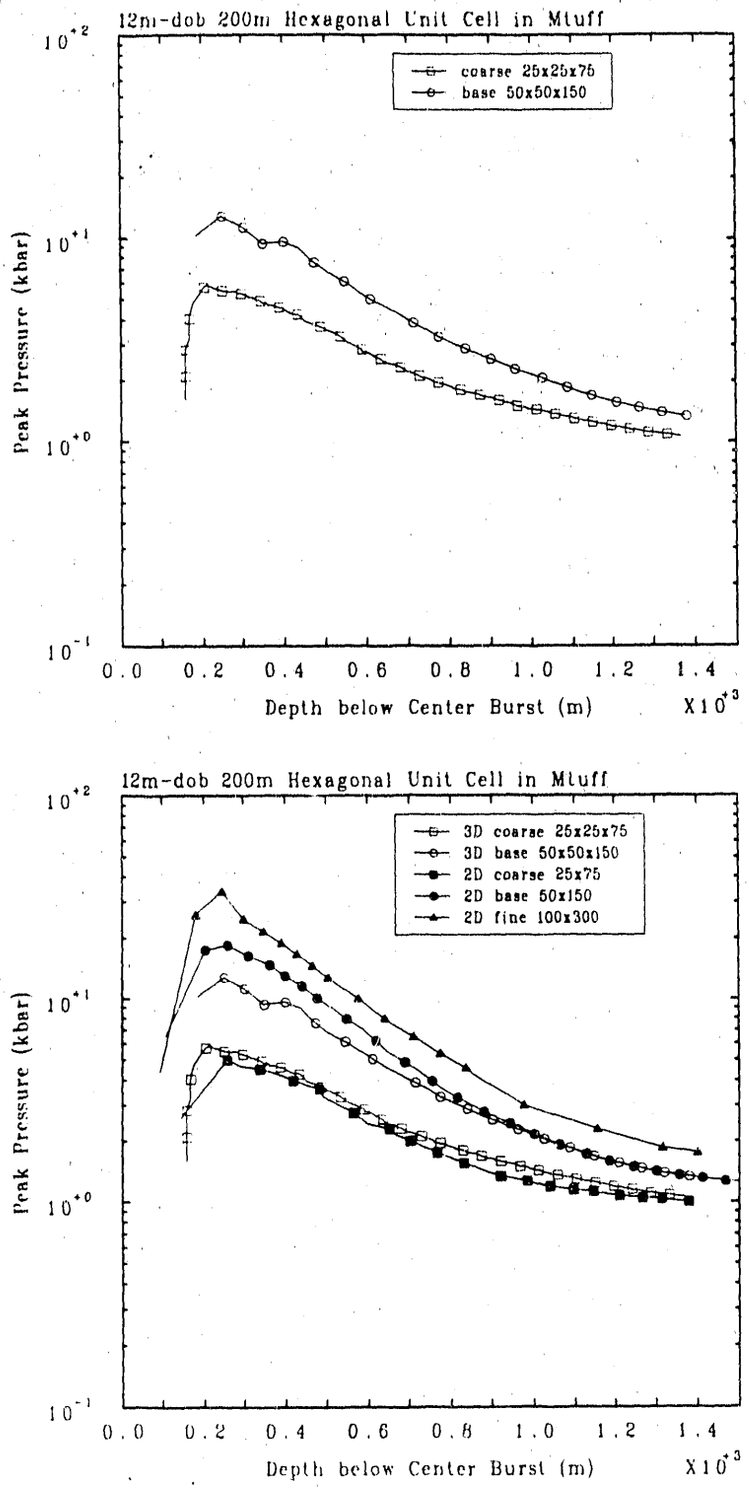

Figure 4.6. Peak Pressure versus Depth for Hexagonal-Unit-Cell Zoning Study Calculations (top) and with Circular-Unit-Cell Results Added (bottom)

5. Finite Array Calculations

The unit-cell calculations, whether for the 2D or the 3D geometry, share a common limitation in that they represent or approximate, in the 2D case, effects of an *infinite* HCP multiburst array. In particular, the reflecting walls of the unit-cell continue to channel energy in the downward direction throughout the calculation, rather than allowing it also to disperse in the lateral direction as it would for a *finite* multiburst array. Nevertheless, as will be shown below, unit-cell calculations can give good estimates of multiburst effects directly beneath the array, at least for moderate depths in the target. Furthermore, since the unit-cell calculations generally require less storage and computing time than do calculations which model the full multiburst array, they are attractive for performing sensitivity studies on various parameters of the problem, *e.g.*, weapon spacing.

To properly represent ground shock effects from a finite multiburst array, 3D calculations are required which follow the waves to great distances in both depth and range. In order to have adequate resolution through all stages of such a calculation, without prohibitive demands on computational resources, special problem initialization and rezoning features were used for the calculations. This section of the report discusses our approach and presents results for finite HCP array calculations. Comparisons will also be made with the unit-cell calculational results reported above. The HULL input model for the finite HCP array is described in Appendix A.3.

5.1 Baseline Study

In general, there is a period of time after detonation of weapons in a multiburst array when the shocks from the bursts will propagate independently of each other. The length of this period depends on the timing, spacing, and yield of the bursts, as well as the target geology. During this phase of the problem, the bursts can clearly be modelled as separate, 2D axisymmetric events. Accordingly, in the HULL finite multiburst array calculations, the 3D wave-interaction part of the problem was initiated by inserting results from well-resolved 2D calculations for the separate bursts into the 3D mesh, with the appropriate spacing and timing to represent the array.

The geometry of the *baseline* calculations for the finite array is shown in Figure A.5, where the weapon spacing was taken to be 400m. The bursts were assumed to be simultaneous in the baseline study. With the assumptions of uniform spacing and simultaneous detonations, the symmetry of the problem is such that only one quadrant needs to be modelled in the calculations, as shown in Figure A.6. Thus, all or portions of only three of the bursts are included in the calculation. The region of the problem that

was modelled in the calculation and the location of the symmetry planes are as indicated in that figure.

From a 2D calculation for one of the bursts, it can be seen that wave interactions for the baseline problem will not have occurred before 20ms after detonation. Thus, to initiate the 3D part of the calculation, results at 20ms from a 2D calculation (for a 500kt burst at 12m DOB) were mapped into the 3D grid at three locations, as shown in Figure A.6.

Figure 5.1 shows the pressure contours on the two vertical coordinate planes, *i.e.*, the x-z and y-z planes, at a sequence of times during the baseline 3D finite array calculations. The complexity of the shock interactions that occur for the multiburst array is apparent in these plots. Notice the development of a coalesced wavefront of fairly large radius due to the shock interaction and reinforcement processes.

Figure 5.2 shows pressure contours on a horizontal plane at ~250m depth, where the quarter-space calculational results have been doubly reflected about x=0 and y=0 to better illustrate the symmetry of the HCP array. Figure 5.3 shows similar results on a horizontal plane at a depth of ~500m. Because of target extent and weapon delivery uncertainties, the lethal "footprint", or area covered by a lethal level of ground shock, is clearly important for assessing weapon effectiveness against buried targets, and Figure 5.4 shows the 0.5kb "footprint" from the present calculations on target planes at depths of ~500m and ~750m.

5.2 Calculation Comparisons

Finite Array versus Single Bursts

Figure 5.5 compares peak pressure versus depth on axis below a single EPW burst, and below the central burst in an HCP array, for:

1. a single 500kt burst,
2. a single 3.5Mt burst,
3. a single 20Mt burst, and
4. a finite HCP array of seven 500kt bursts with 400m burst separation..

The 500kt single burst results were obtained from the present 3D finite array calculations by identifying the effects associated with the leading wave for the single, central burst in the array, while the curves for the 3.5Mt and 20Mt single bursts were scaled from the 500kt results. Thus, equivalent zoning was used for all results shown in the figure. It can easily be seen that, in terms of the peak pressure below the center of the array, the

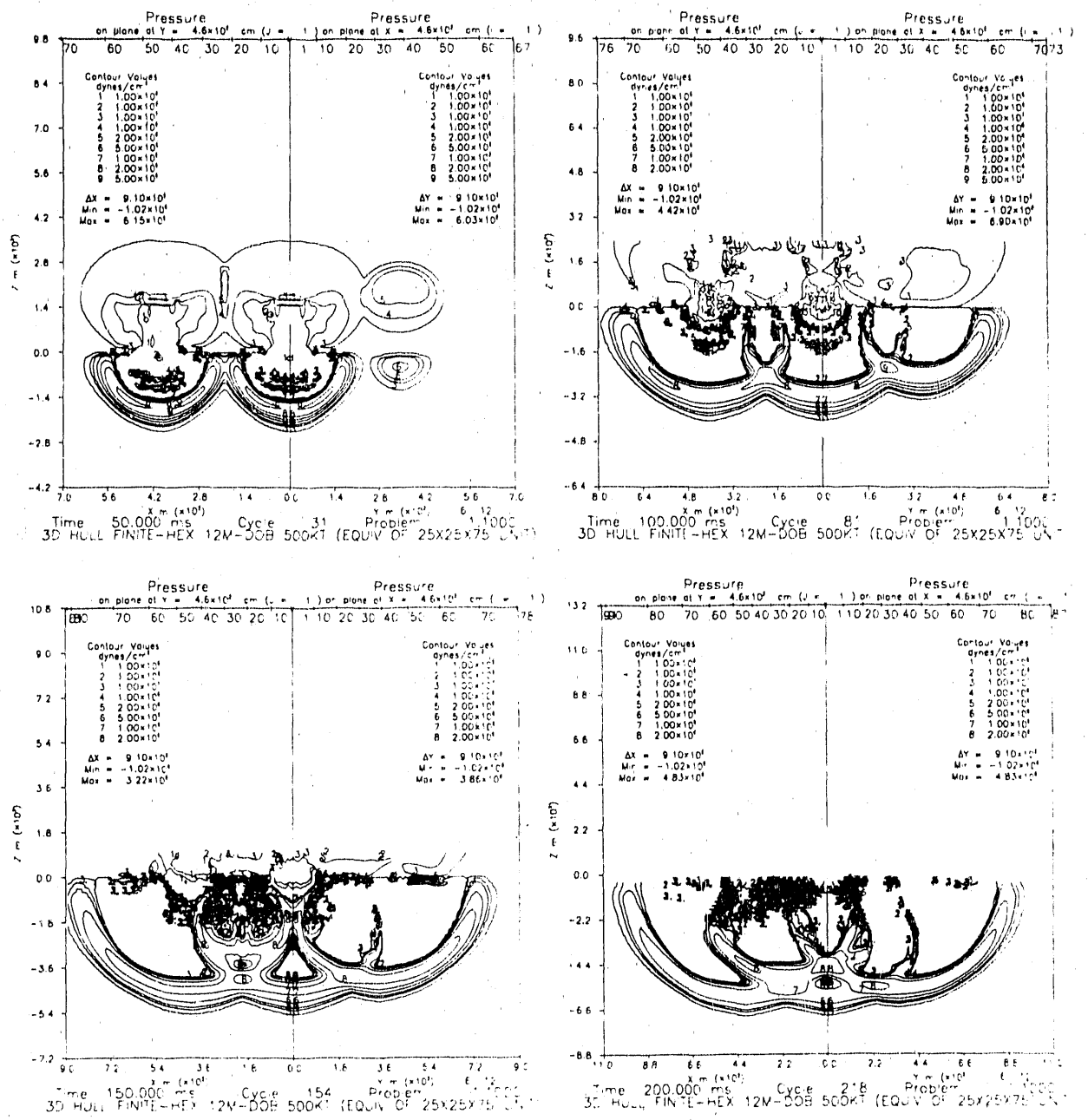

Figure 5.1. Pressure Contours (split-frame: (x-z) plane on left and (y-z) plane on right) for Finite Array Calculations at Problem Times of 50ms (top left), 100ms (top right), 150ms (bottom left), and 200ms (bottom right)

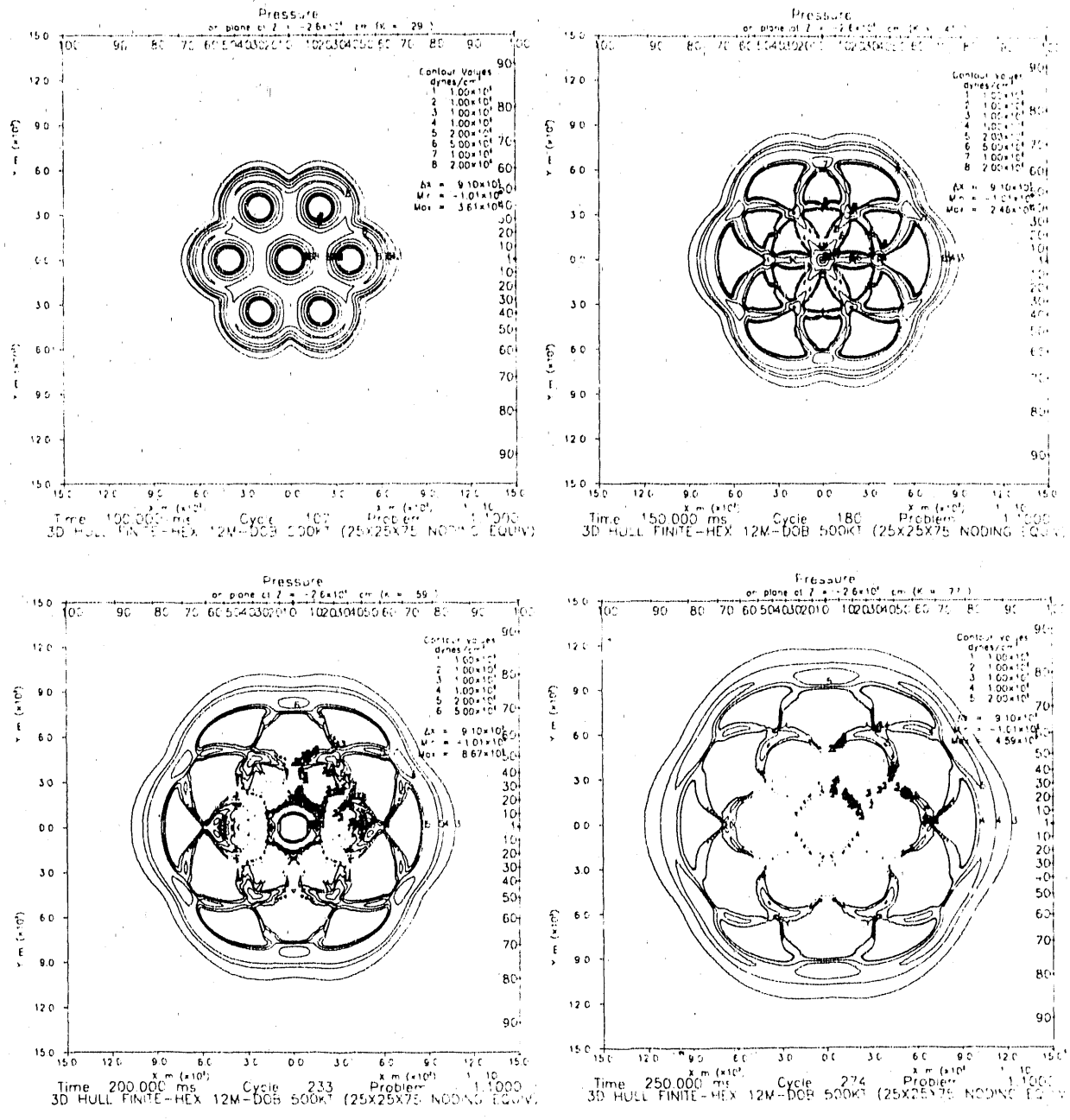

Figure 5.2. Pressure Contours on Horizontal Plane at ~250m Depth for Finite Array Calculations at Problem Times of 100ms (top left), 150ms (top right), 200ms (bottom left), and 250ms (bottom right)

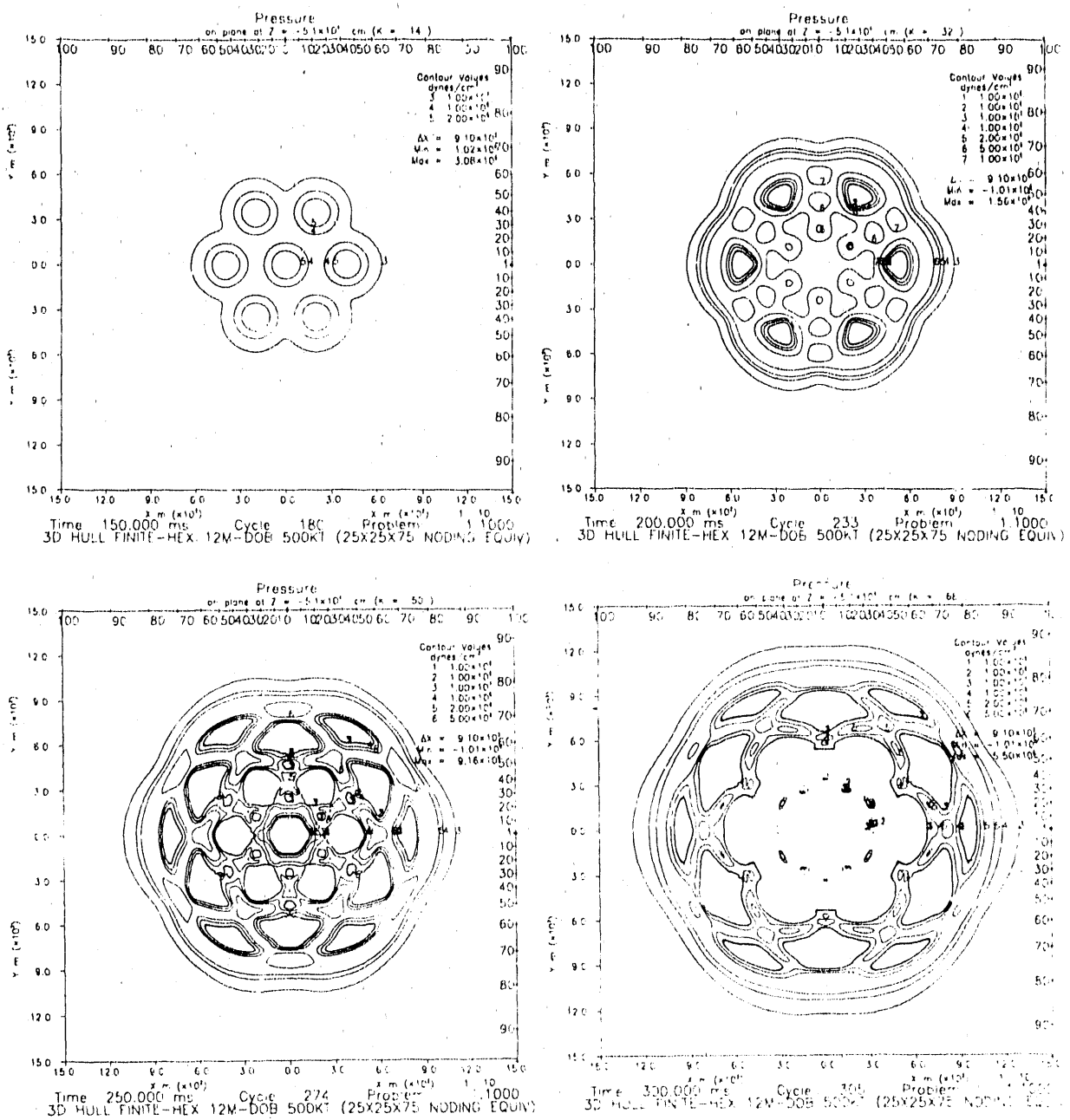

Figure 5.3. Pressure Contours on Horizontal Plane at ~500m Depth for Finite Array Calculations at Problem Times of 150ms (top left), 200ms (top right), 250ms (bottom left), and 300ms (bottom right)

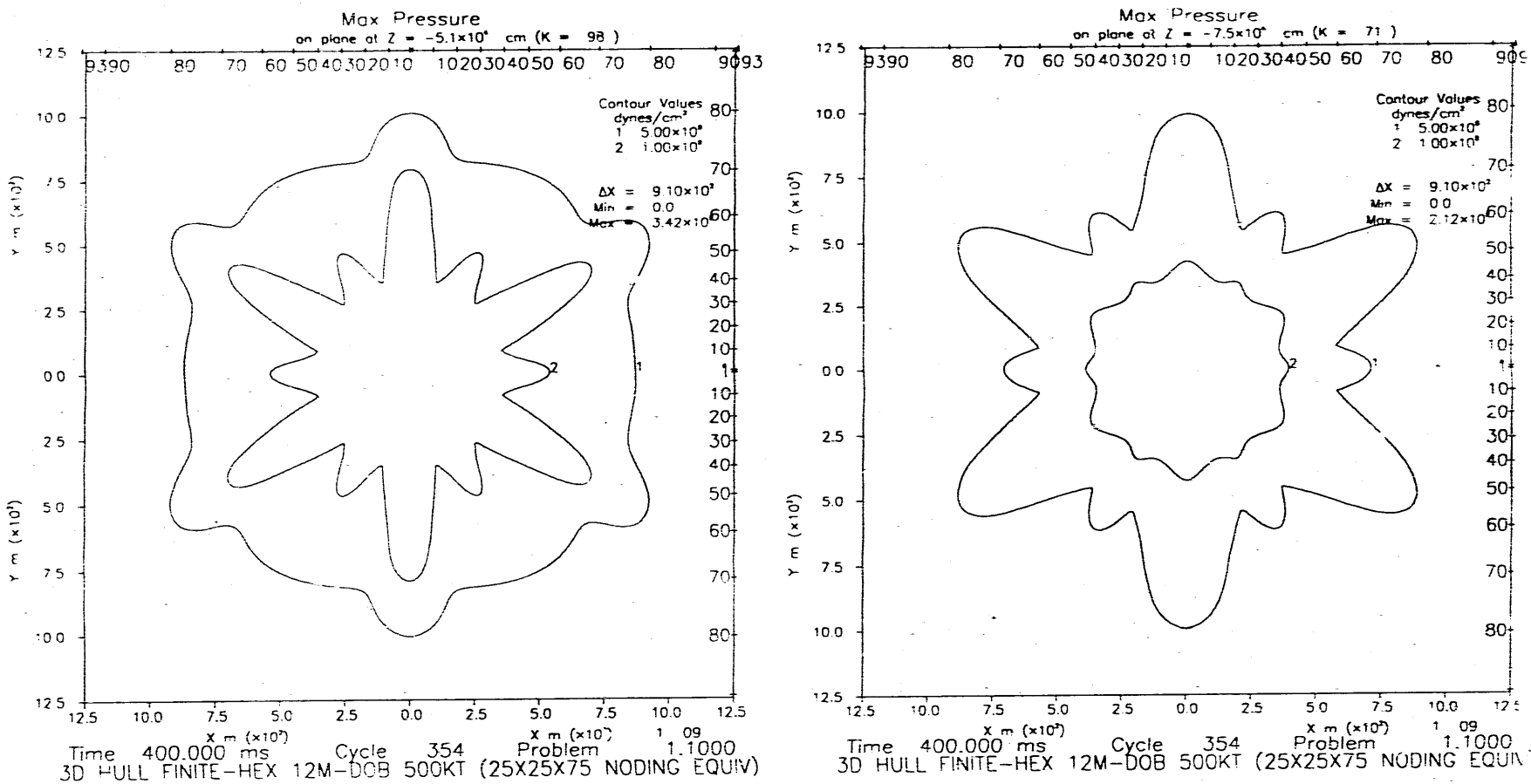

Figure 5.4. Peak Pressure Contours ("Footprints") on Target Planes at ~500m Depth (left) and ~750m Depth (right) for Finite Array Calculations (Contour 1: 0.5kb, Contour 2: 1.0kb)

multiburst scheme delivers a stronger ground shock than the single 3.5Mt burst of the same total, or *aggregated*, yield. In fact, as was seen in the earlier unit-cell calculations, the results in Figure 5.5 suggest that the ground shock on axis for the array would be equivalent to a single burst of 20Mt. Thus, on a constant *aggregated yield* basis, this corresponds to an increase of ~80% in depth-to-effect at the 0.5-1.0kb level.

3D Finite Array versus Unit-Cell Analyses

It is interesting to compare results for the finite array and unit-cell calculations. Accordingly, results of the *baseline* hexagonal-unit-cell calculation are added in the bottom plot of Figure 5.5. The agreement is seen to be very good. It should be noted that the zoning and rezoning procedures used in the unit-cell and finite array calculations were such that zone sizes were equivalent for those calculations in the region below the array. Thus, we conclude that the unit-cell calculations provide a good approximation to multiburst effects for peak pressure directly below the array.

5.3 Timing Sensitivity Study

An additional calculation was done to investigate the effect on ground shock of non-simultaneity (*i.e.*, timing "jitter") between the detonations in the seven-burst array. In particular, it was assumed that, relative to the weapon at the center of the array, two of the outer weapons (at diametrically opposite locations) detonated 20ms late, while the other four detonated 10ms early. Accordingly, to initialize the 3D part of the problem, results from a 2D, single-burst, calculation at 10ms, 20ms and 40ms were used at the appropriate locations in the 3D grid, as shown in Figure A.7. A nominal problem time of 25ms was assigned for startup of the 3D part of the problem, and pressure contours at that time in the plane of the burst are shown in Figure 5.6.

Figure 5.7 shows peak pressure below the center of the burst array, for the baseline calculations and for those which modeled the non-simultaneous bursts. The effect of the timing jitter is to reduce the peak pressure delivered to a given depth below the center of the array, since disturbances from the surrounding bursts reach the centerline at different times. The reduction in peak pressure decreases from a factor of ~2 at higher pressure levels to a factor of ~1.1 at pressure levels of 1kb.

In addition to degrading the peak pressure on axis, the timing jitter also reduces the size of the lethal footprint for the array. For example, Figure 5.8 shows the 0.5kb and 1.0kb footprints on the target plane at 750m depth, and Figure 5.9 compares results for the calculations with and without timing jitter.

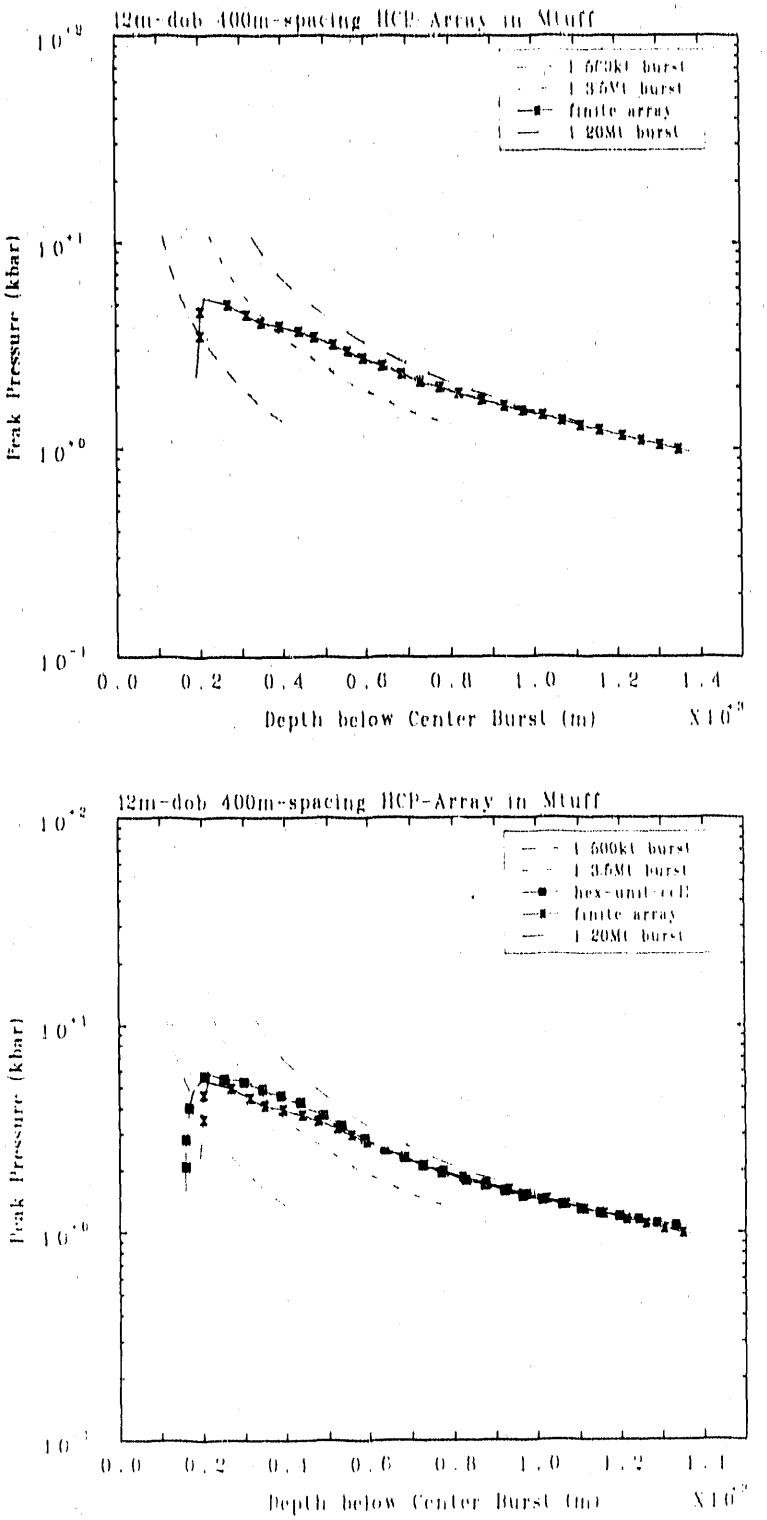

Figure 5.5. Peak Pressure versus Depth for Finite Array Calculations Compared with Single Burst Results (top) and with Hexagonal-Unit-Cell Results Added (bottom)

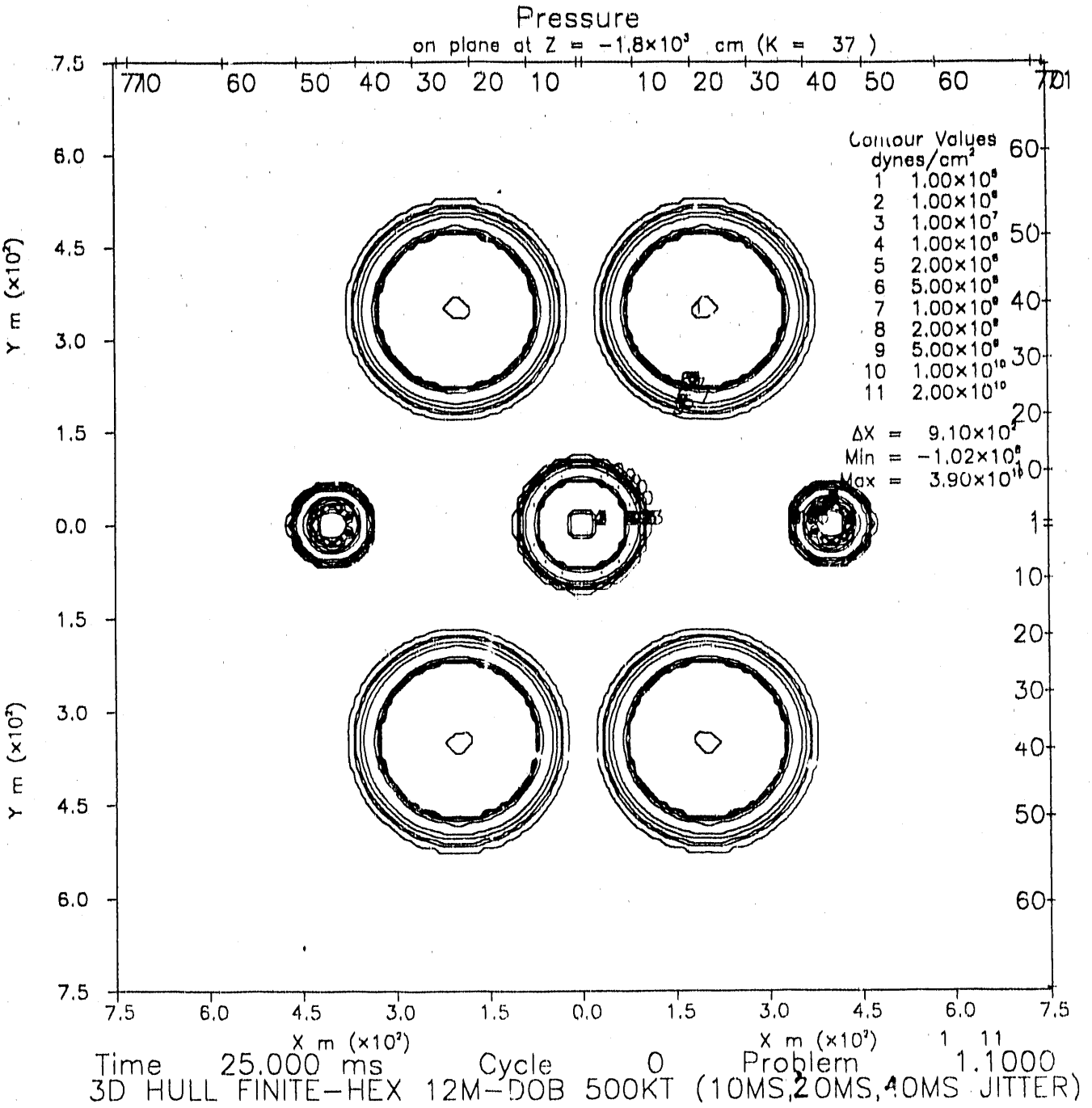

Figure 5.6. Pressure Contours (in plane of bursts) at Beginning of 3D Calculations for Asynchronous HCP Array

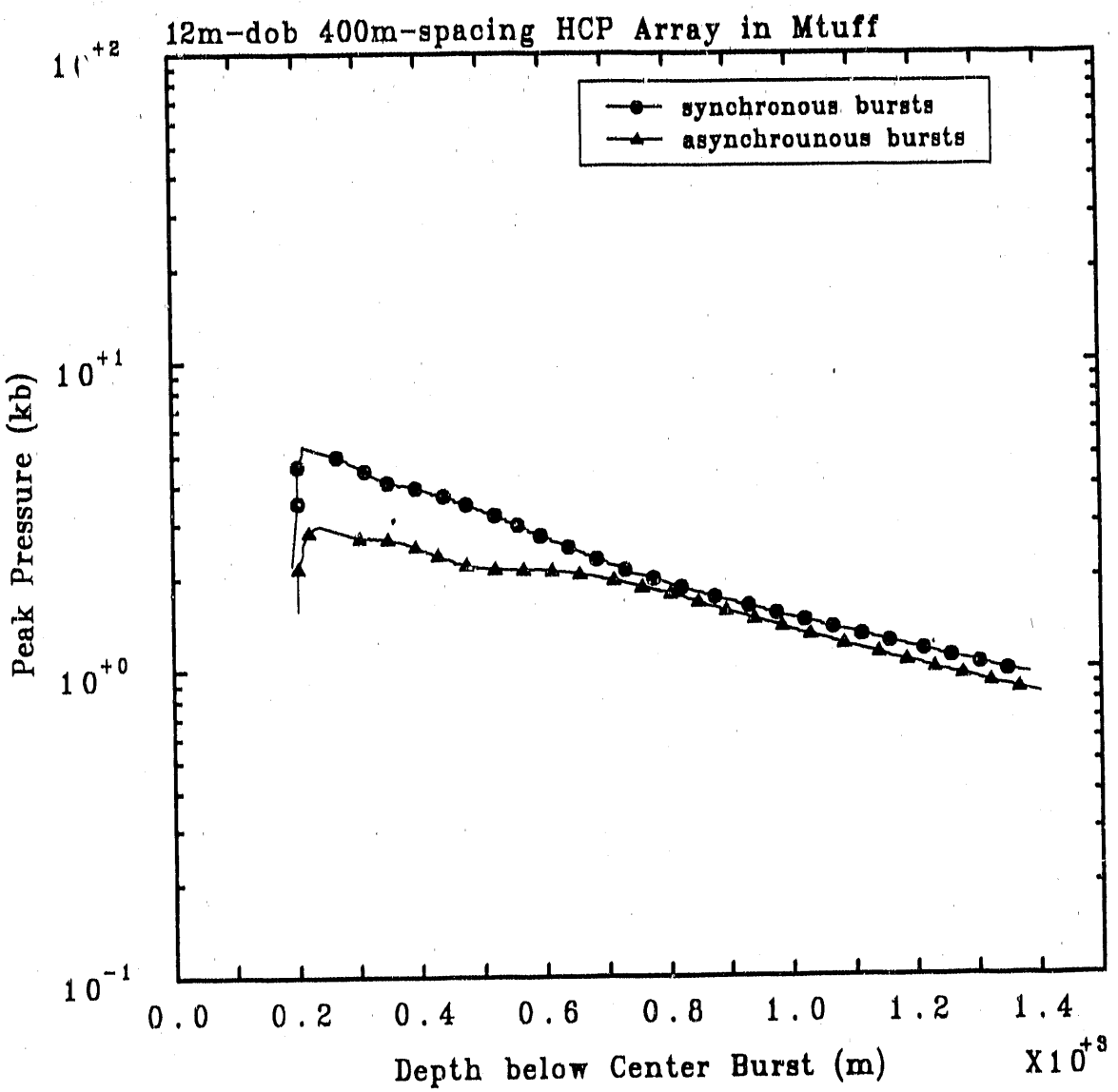

Figure 5.7. Peak Pressure versus Depth for Synchronous and Asynchronous Bursts in Finite HCP Array

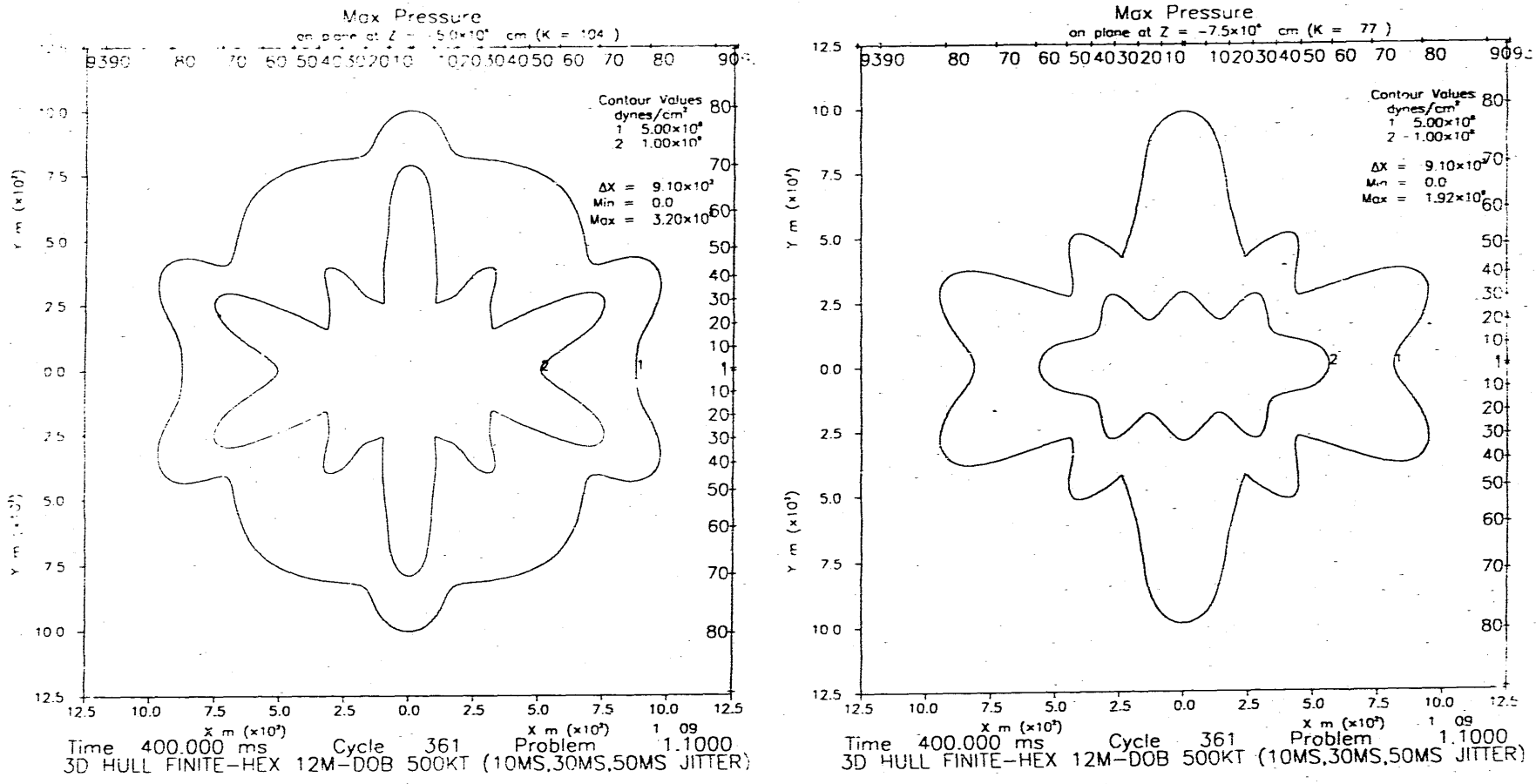

Figure 5.8. Peak Pressure Contours ("Footprints") on Target Planes at ~500m Depth (left) and ~750m Depth (right) for Asynchronous Finite Array Calculations (Contour 1: 0.5kb, Contour 2: 1.0kb)

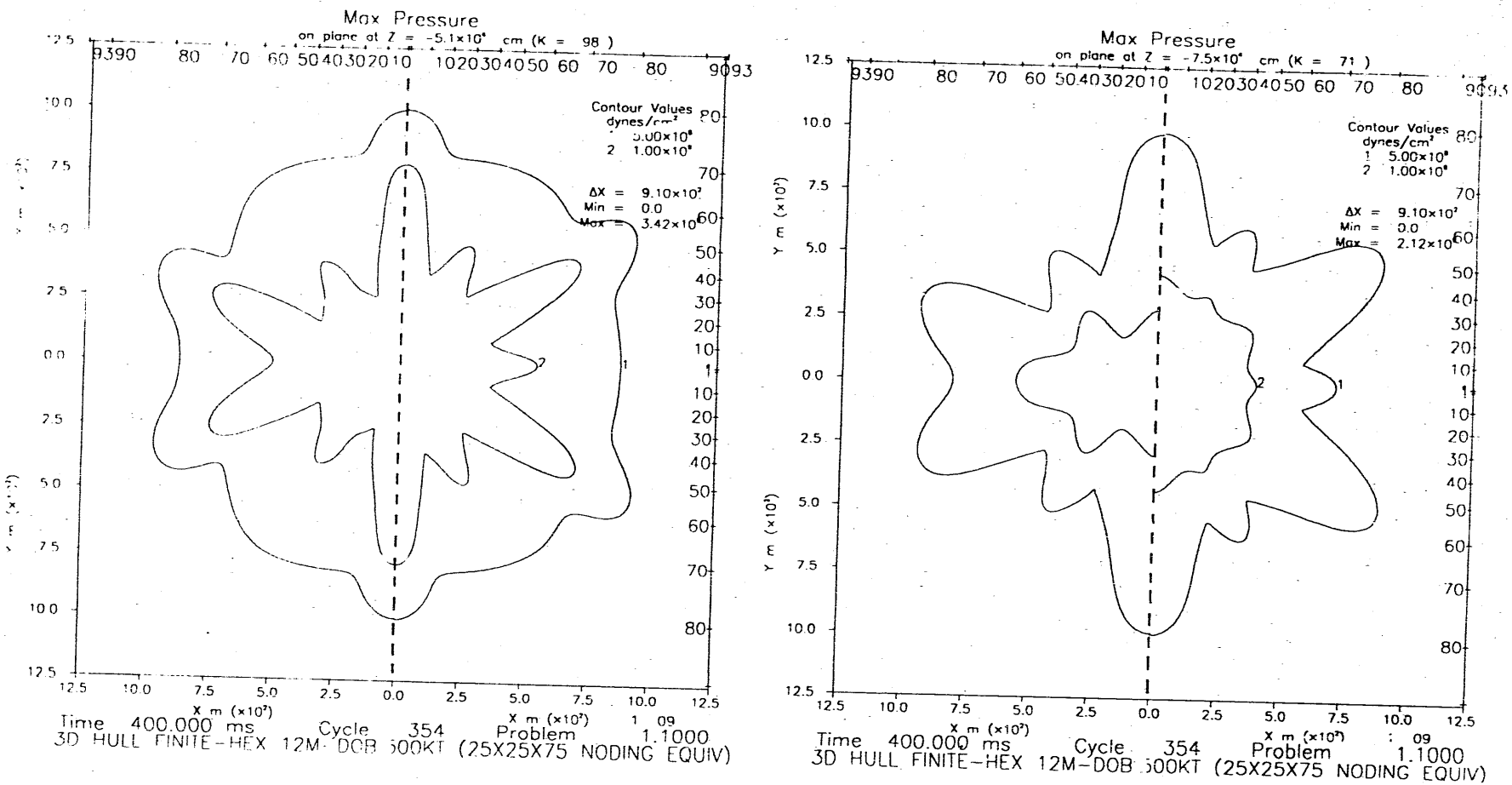

Figure 5.9. **Peak Pressure Contours ("Footprints") on Target Planes at ~500m Depth (left) and ~750m Depth (right) for Finite Array Calculations (Contour 1: 0.5kb, Contour 2: 1.0kb; Split-frame plots show results for asynchronous bursts on left and synchronous bursts on right)**

6. Discussion and Conclusions

This report presents results of two-dimensional (2D) and three-dimensional (3D) HULL hydrocode calculations that simulate ground shock effects from detonations of multiple earth penetrator weapons arranged in hexagonal-close-packed (HCP) arrays. The calculations simulated both: 1) an array involving a large number of weapons, *i.e.*, an effectively infinite array, and 2) a finite array of seven bursts. The EPWs in the array were each assumed to have a nominal yield of 500kt, a depth-of-burst (DOB) of 12m, and a baseline spacing of 400m. Various other spacings were considered in sensitivity studies. The target material was modeled as a homogeneous, wet, soft rock.

For the case in which there is a large number of weapons in the HCP array, *i.e.*, an effectively infinite array, the problem can be simulated by analysis of effects in a unit-cell of hexagonal cross-section, which is centered on one of the bursts and extends cylindrically in the axial direction above and below it. The hexagonal-unit-cell calculation is a 3D problem, which can be approximated by using a circular-unit-cell to define the reflective unit-cell boundary. This approximation then permits 2D analysis of the problem.

Results for the unit-cell calculations indicate that the circular-unit-cell (2D) approximation overpredicts the peak ground shock stress levels in the higher pressure regimes relative to the hexagonal-unit-cell (3D) calculations. The 2D problem, however, is seen to become a very good approximation to the 3D case at depths below the array that are about twice the charge separation distance. For the arrays considered here, peak stresses at that depth were below a few kilobars in magnitude. In terms of peak pressure below the bursts, the unit-cell results suggest that an HCP array of 500kt EPWs is equivalent to a single burst of 20Mt, or about six times the *aggregated yield* of the seven-burst array.

The unit-cell calculations have the limitation that they can only represent, to some approximation, effects of an *infinite* HCP array. In particular, those calculations continue to channel ground shock energy in the vertical direction throughout the problem, rather than allowing it to disperse in the lateral direction, as would be the case for a *finite* multiburst array. Therefore, to complete this study, 3D calculations were performed which simulated the interaction of ground shock effects from a *finite*, seven burst HCP array. Conditions of both simultaneous and non-simultaneous detonation of the bursts were considered.

All indications from the calculations in this study are that a seven burst HCP array can increase by ~80% the depth to which a specified overpressure level (*e.g.*, 1kb) is delivered to the target, when compared with effects for a single burst of the same total, or *aggregated*, yield. The calculations also showed that, for a seven burst HCP array of

500kt EPWs, the 0.5kb footprint on a plane at 500m depth covers an area greater than one square kilometer. Furthermore, this coverage can be achieved even with a timing jitter of as much as 20ms between the detonations.

These studies have demonstrated that the HULL code is a useful tool for multiburst ground shock analyses, and the calculational results suggest that multiburst schemes are a possible means of achieving the ground shock effects of a large yield EPW from a number of smaller-yield weapons. Our future studies in this area will focus on more realistic weapon arrays, *viz.*, fewer weapons and smaller yields, and on generating a calculational database for development and benchmarking of simplified methods (*e.g.*, linear superposition techniques) for predicting multiburst effects.

References

[1] Matuska, D. A. and J. J. Osburn, "HULL Documentation Volume I: Technical Discussion; Volume II: Users Manual", Orlando Technology, Inc., Shalimar, Florida.

Appendix A
HULL Input Model Descriptions

A.1 Circular-Unit-Cell (2D) Calculational Model

In the baseline 2D axisymmetric unit-cell calculations, an (x-y) grid of 50×150 zones was used, with square zones 25cm on a side. The x=0 boundary is automatically a symmetry, or reflecting, boundary in 2D axisymmetric-cell calculations. The region covered by the initial zoning is shown in Figure A.1.

The automatic rezoning option was used to extend the initial zoning region and follow the expanding spherical shock front during the problem. As the zones expanded beyond the original mesh, they were filled with either tuff or air, as appropriate, at ambient conditions.

The rezone was "triggered" by a non-zero velocity and/or non-ambient pressure in any cell adjacent to the right, top, or bottom boundary. When triggered by the outer radial boundary, the expanding rezoner increased the cell size in both the axial and radial directions by 5%. The x=0 symmetry boundary was always held fixed. If either the top or bottom (axial) boundary triggered the rezone, the opposite y-boundary was held fixed, while increasing the cell size in the axial and radial directions by 5%.

The expanding rezoner was used to follow the shock front until it reached the edge (radius) of the unit-cell for the problem, at which time a reflecting boundary was inserted to represent the cell boundary. The reflecting boundary was implemented by setting the mass and energy in the outer radial zones to zero, thus invoking the HULL rigid-body, or "island", logic. This option was explained in Section 2. Although the standard HULL reflecting boundary condition could have been applied more easily to define the edge of the unit-cell, the above procedure was followed in order to be able to use the same approach to define unit-cell boundaries in both the 2D *and* 3D calculations. In the latter case, portions of the unit-cell boundaries do not follow calculational grid lines and, therefore, cannot be treated with the standard reflecting boundary condition. The 3D unit-cell calculations will be discussed in the next section.

After the wave reached the edge of the unit-cell, and the reflecting outer boundary had been inserted, the *expanding* rezoner was no longer needed. At that point, a *translating* rezoner was used to follow the shock as it propagated downward into the target. The rezoner was triggered by a non-zero velocity in any cell along the bottom boundary. This translating rezoner kept the cell size fixed, but shifted the mesh in the vertical direction, downward, at a ~5% rate, discarding material at the top of the mesh,

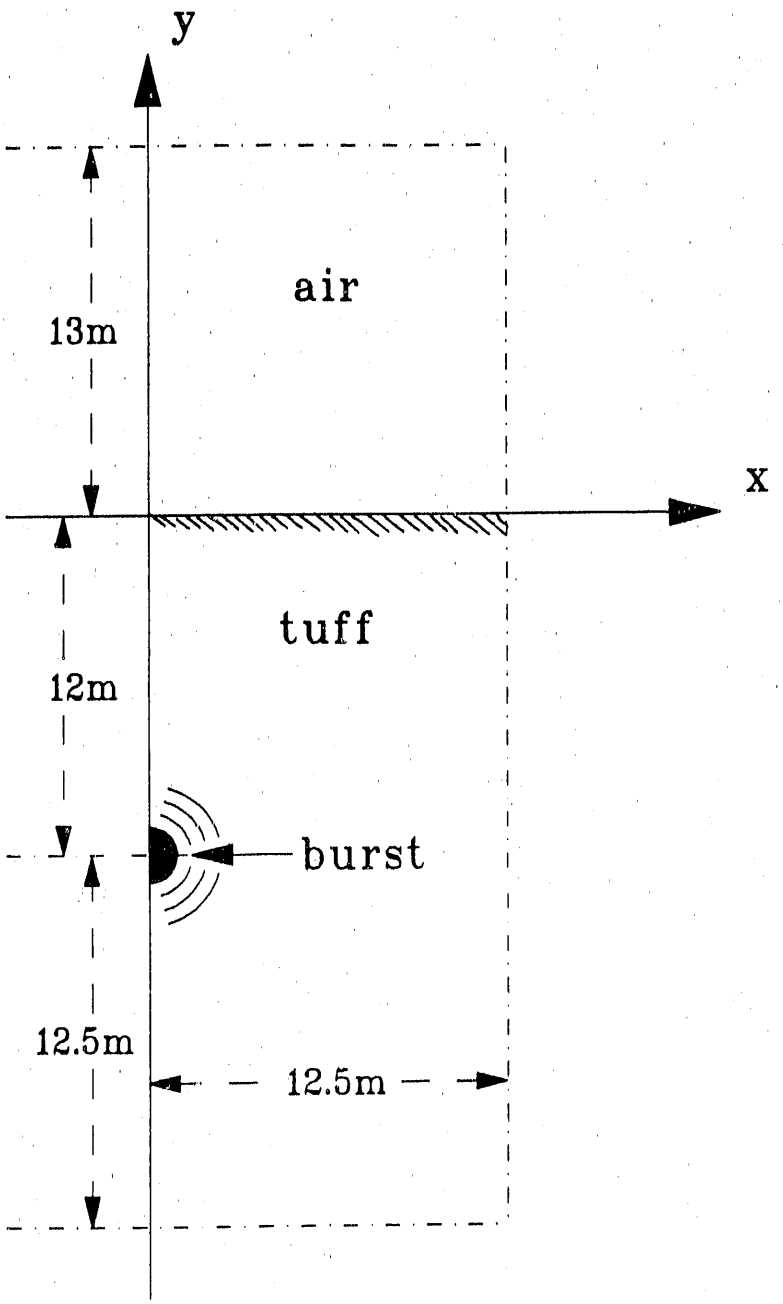

Figure A.1. Initial Zoning Region for Circular-Unit-Cell Calculations

as required.

Additional 2D unit-cell calculations were done with a more finely-zoned (100×300) and a more coarsely-zoned (25×75) grid, *i.e.*, calculational grids with, respectively, twice and half the number of zones in each direction as were used in the baseline calculations. The finely-zoned problems were begun with square zones 12.5cm on each side, while the coarsely-zoned problems were begun with square zones 50cm on each side. The initial mesh, in both cases, extended 12.5m in the x-direction and 37.5m in the y-direction, as shown in Figure A.1.

A.2 Hexagonal-Unit-Cell (3D) Calculational Model

Three-dimensional calculations were done to model the hexagonal-unit-cell shown in Figure 1.2. An (x,y,z) grid of 50×50×150 zones was used in the baseline calculations for this problem. The zones were cubical and 25cm on a side at the beginning of the calculation. Due to the symmetry of the problem, only one quadrant of the hexagonal-unit-cell was modelled, as shown in Figure A.2, and reflecting boundary conditions were used at x=0 and y=0. The region covered by the initial grid is shown for the vertical coordinate planes in Figure A.3.

Initially, an expanding rezoner was used to follow the spherical shock front. When triggered by a non-ambient pressure and/or non-zero velocity in any cell at the right, front, top, or bottom boundary, the rezoner expanded the zones by 5% in all directions. This was done while holding fixed the x=0 and y=0 boundaries, and sometimes one of the z-boundaries, depending on which boundary triggered the rezone.

As for the 2D unit-cell calculations described in Appendix A.1, the expanding rezoner was used to follow the shock front until it reached the edge of the unit-cell for the problem. At that time, the reflecting boundary of the unit-cell was defined by setting the mass and energy of boundary zones to zero in the pattern shown in Figure A.4. This procedure invoked the HULL rigid-body, or "island", logic for these zones, as explained in Section 2. After the unit-cell boundary had been inserted in the problem, the rezoning procedure was switched to the translating option, as described in Appendix A.1, and used to follow the shock as it propagated downward into the target.

Calculations were also done with a more coarsely-zoned (25×25×75) grid, where the number of zones in each direction was half that used in the baseline calculations. In this case, the problem was begun with cubical zones of 50cm sidelength, *i.e.*, twice that used for the baseline calculations. (Note that a finely-zoned problem equivalent to that done for the case of the 2D unit-cell calculations, *i.e.*, where the number of zones is *doubled* in each direction over that used in the baseline calculations, was considered impractical in terms of computing time.)

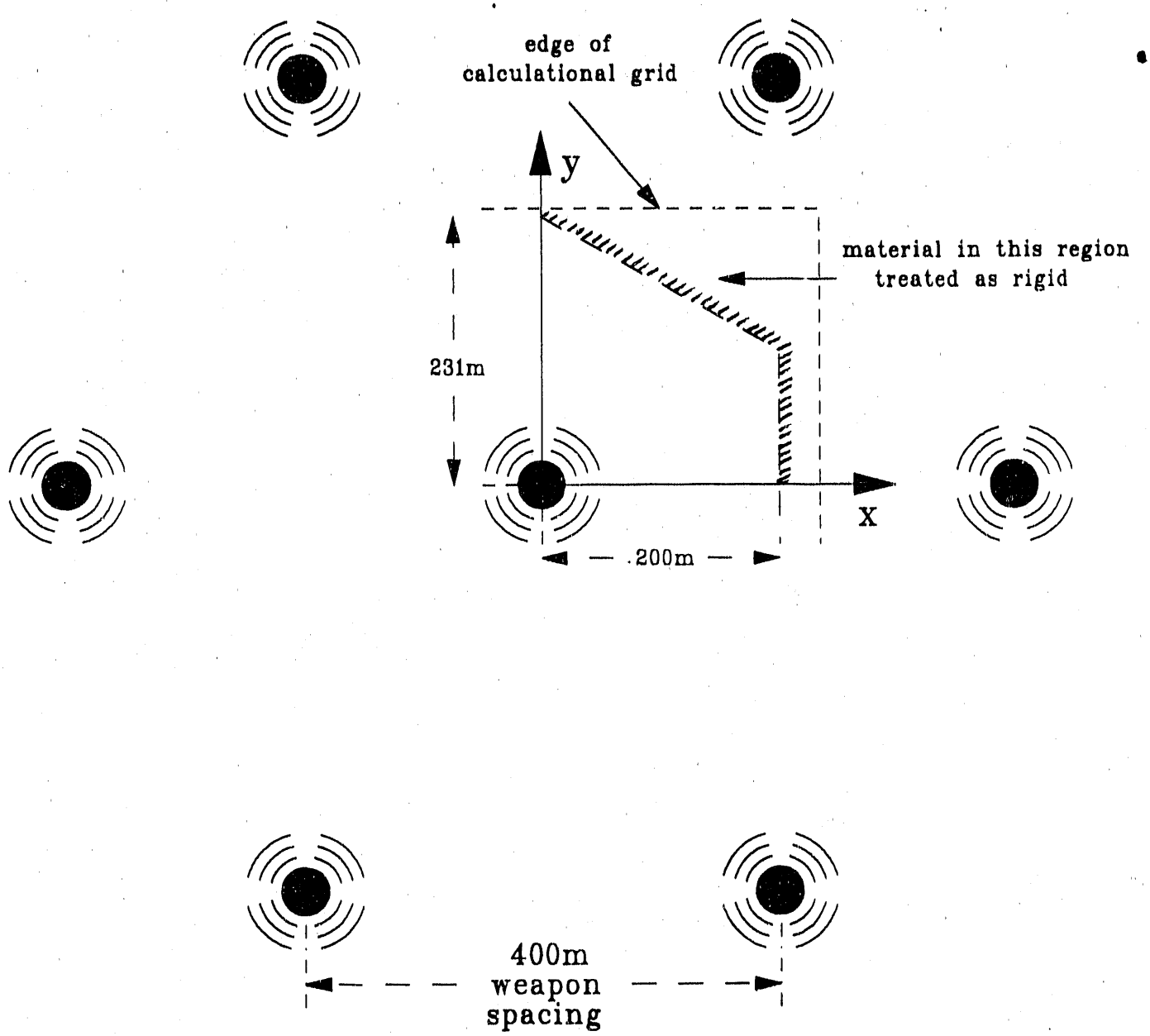

Figure A.2. Cell Boundary Geometry for Hexagonal-Unit-Cell Calculations

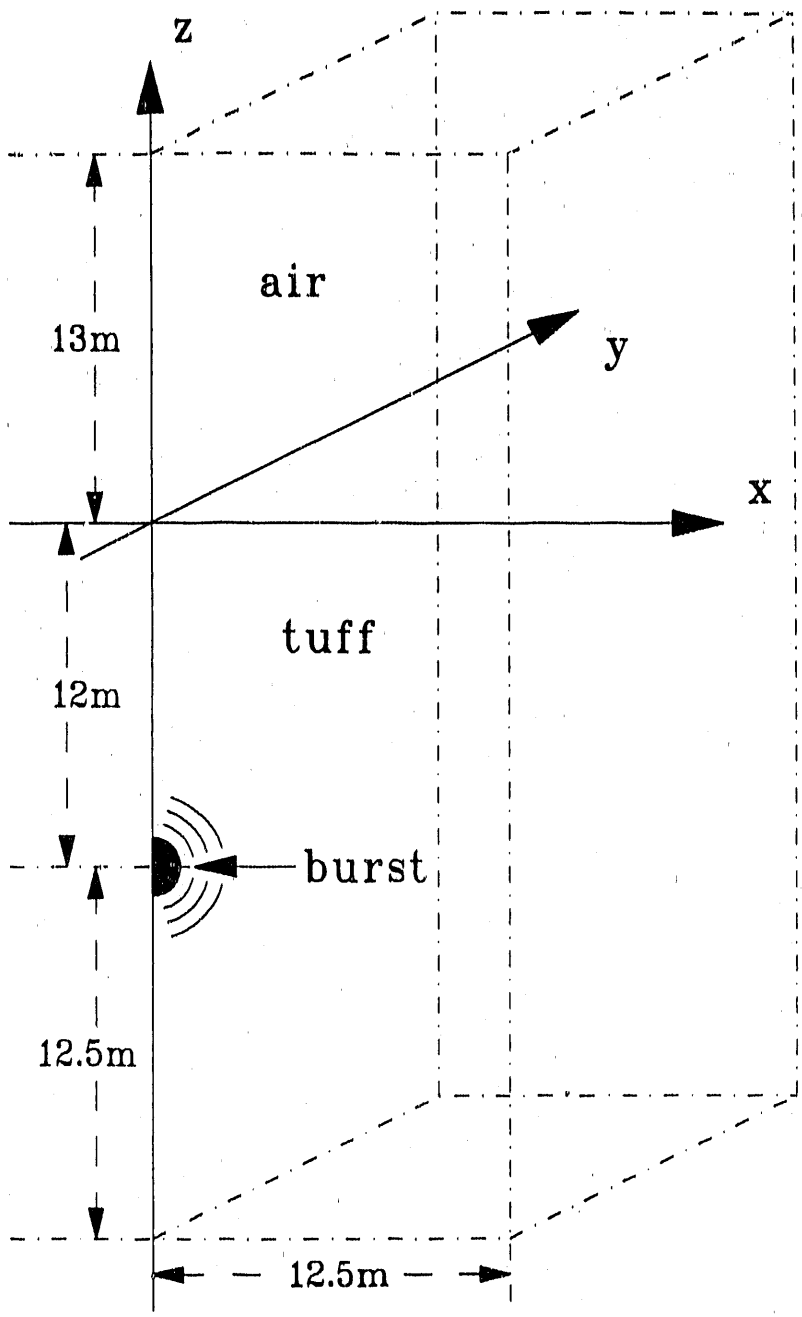

Figure A.3. Initial Zoning Region in Vertical Planes for Hexagonal-Unit-Cell Calculations

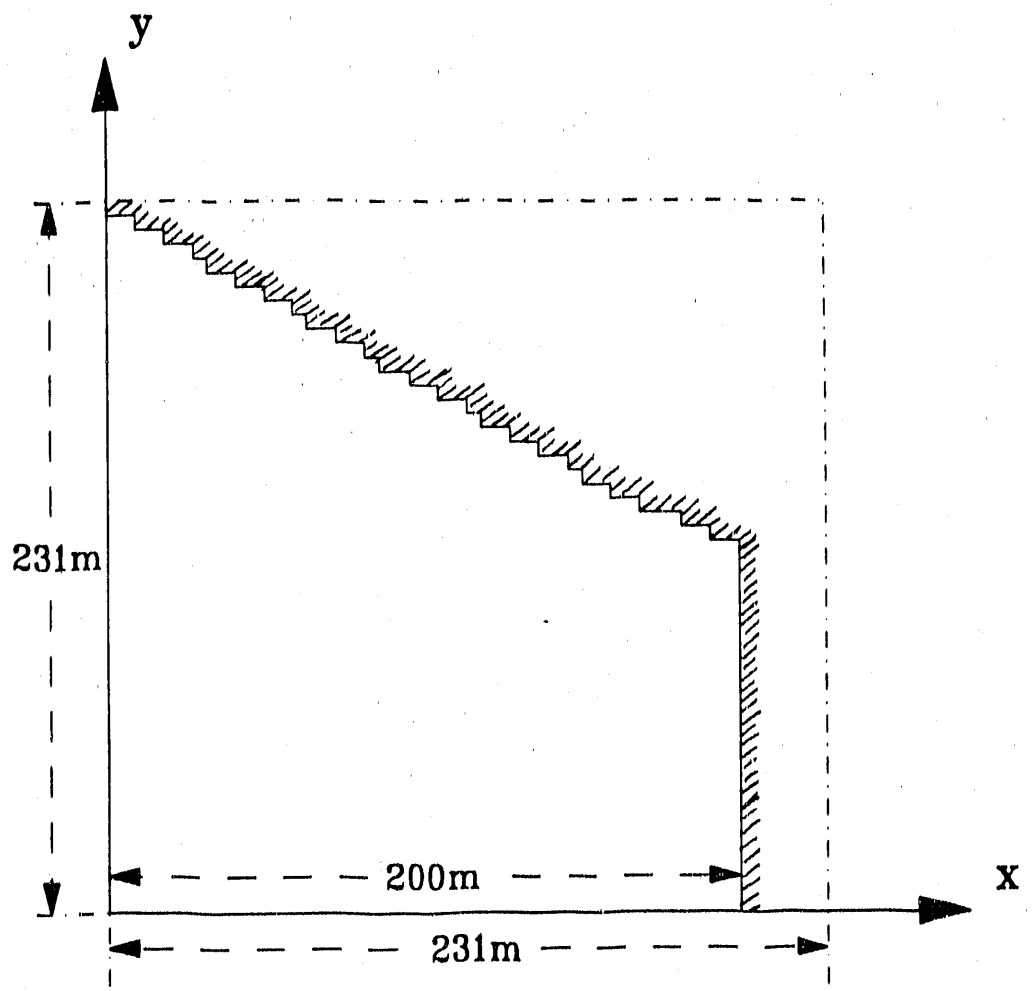

Figure A.4. Reflecting Boundaries for Hexagonal-Unit-Cell Calculations

A.3 Finite Array (3D) Calculational Model

Special computational techniques were required to treat the 3D problem of a *finite* multiburst array, such that adequate resolution would be provided during all stages of the calculation without prohibitive computing costs. For the 3D finite array calculations in the present study, the HULL FIREIN option enabled this to be done. With the FIREIN option, it is possible to insert results of separate, well-resolved 2D calculations for individual bursts into a 3D grid prior to the time at which wave interactions would occur. Variations in spacing and/or timing between bursts can be easily represented by selecting 2D calculational results at *different* problem times to insert at the various burst positions in the *initial* 3D grid.

The first 3D finite array calculation that was done in the present study involved the simultaneous detonation of seven bursts at 400m separation in an HCP array, as shown in Figure A5. For the 2D single-burst calculation that was used to initialize the 3D part of the problem, the zoning and rezoning techniques were the same as were used in the baseline 2D circular-unit-cell calculations. These were described in Appendix A.1. Problem edits from the 2D calculation were then selected at suitable times such that no wave interactions would have occurred between the bursts when inserted at the desired array spacing in the 3D grid. For the case of seven completely synchronized bursts separated by 400m in an HCP array, a common time edit at 20ms from the 2D calculation was used to initialize each burst in the 3D part of the problem.

The initial three-dimensional mesh for the finite array calculations was setup to be just large enough to contain the wave fronts from the several bursts inserted in the grid. Due to the symmetry of the problem, it was possible to use reflecting boundary conditions at x=0 and y=0 and thus model only one quadrant of the problem, as shown in Figure A.6. An (x,y,z) grid of 114×118×125 zones was used, with a constant subgrid of 44×38×100 cubical zones 9.1m on a side. As shown in Figure A.6, the constant subgrid extended 400m in the x-direction and 346m in the y-direction from the array center. An additional 70-80 zones of uniformly increasing size (at a 2.5% rate) were used in the x- and y-directions beyond the subgrid to model further reaches of the target. In the z-direction, the constant subgrid was 910m in length, with 350m of the grid below the ground surface and 560m in the air region. An additional 25 zones of uniformly increasing size (at a 2.5% rate) were used in the z-direction above the subgrid.

After the 3D calculations were initiated and the wave interactions between the bursts had just occurred, a translating rezoner (which kept the cell sizes fixed in both the constant subgrid and surrounding regions of the mesh) shifted the mesh vertically downward at a 5% rate, whenever triggered by a non-zero velocity or non-ambient pressure in a cell along the the bottom boundary. With 100 zones in the z-direction in the constant subgrid, more than 900m of vertical resolution was provided to follow the shock front downward into the ground. (The *radial* growth of the ground shock was accomodated by the 70-80 zones of increasing size that were used in the x and y-directions beyond the subgrid).

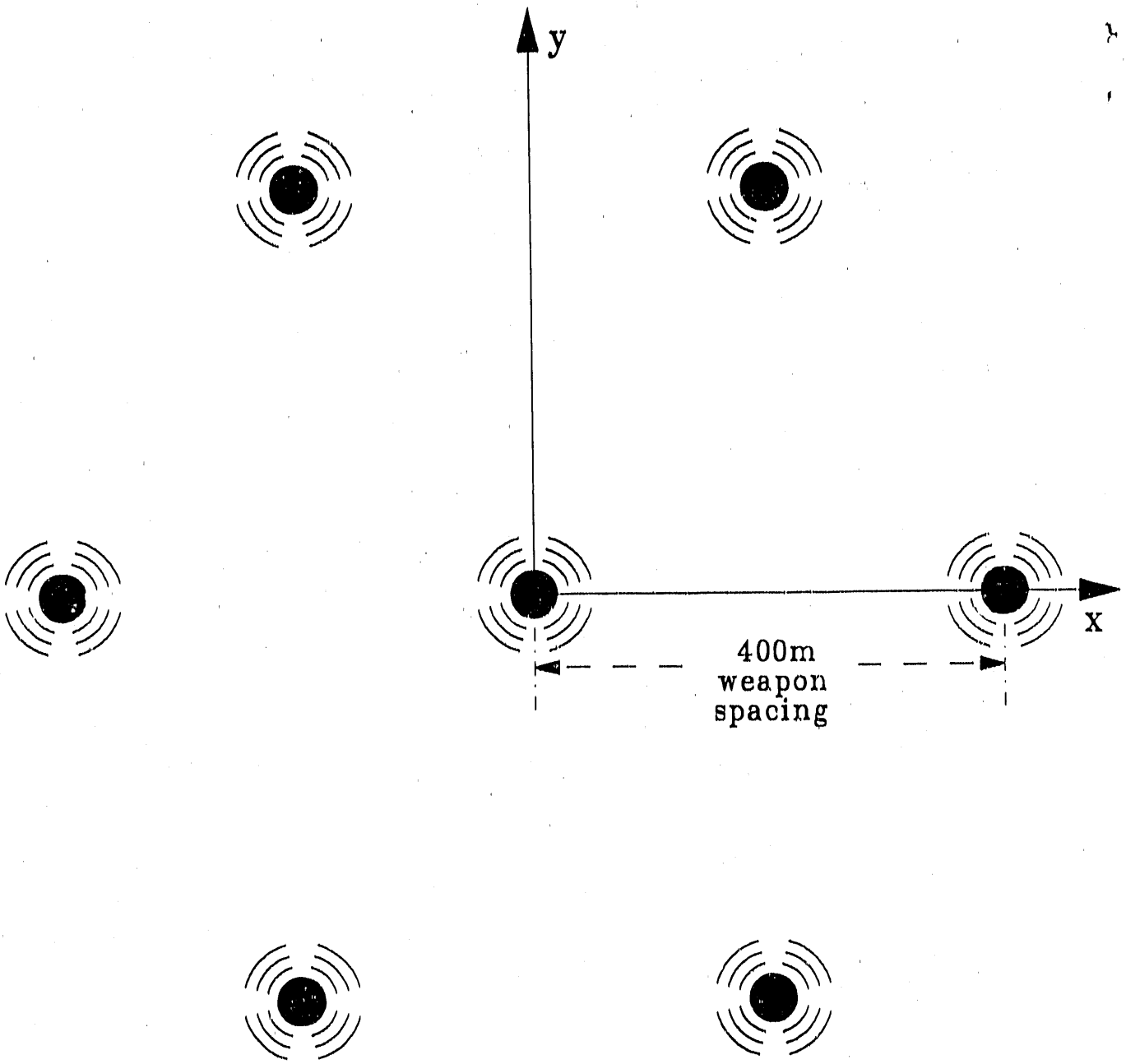

Figure A.5. Burst Positions for Finite HCP Array

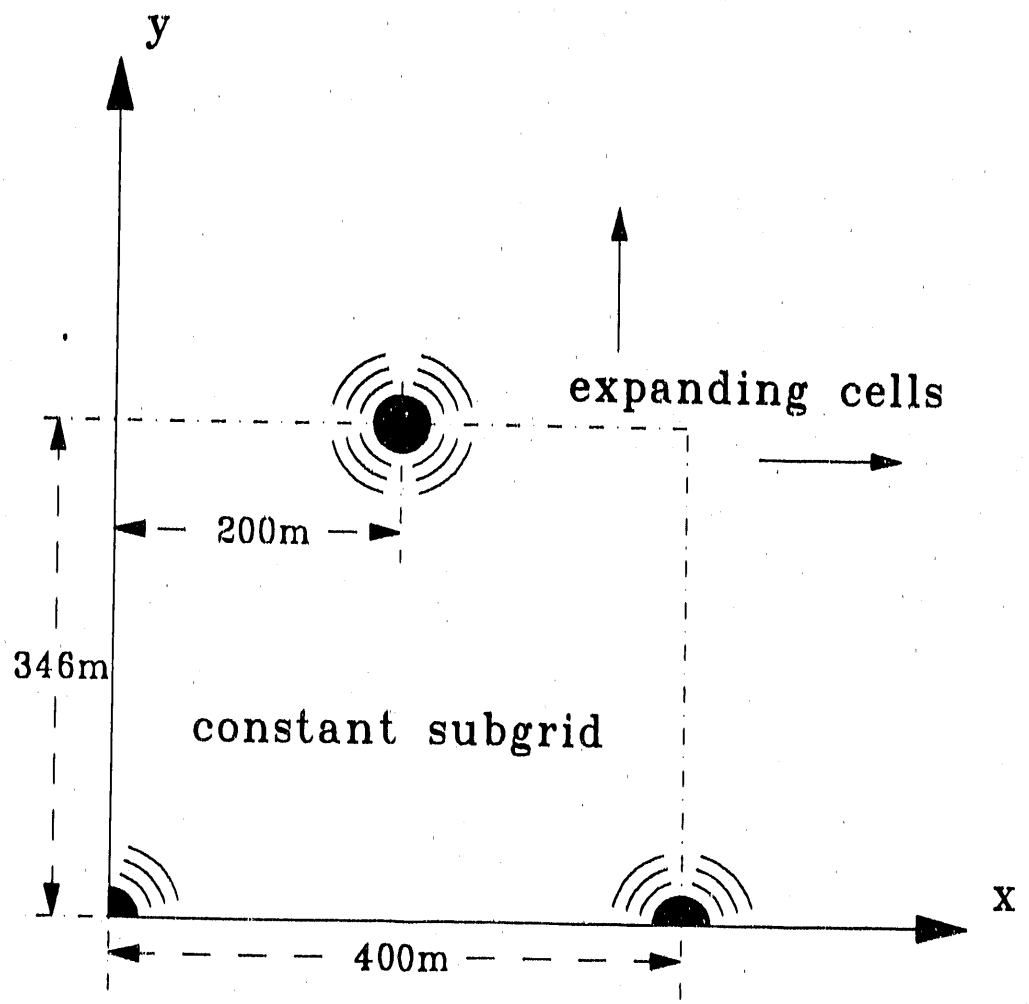

Figure A.6. Quarter-Space for Finite Array Calculations

The reason for maintaining and translating the constant subgrid region in the *finite* array calculations was to ensure that the zoning in the principal, wave-reinforcement region, *i.e.*, the region directly beneath the array, would be the same as the zoning used in the hexagonal-unit-cell, or *infinite* array, calculations. Thus, in comparing ground shock effects for those two cases, effects of zoning differences would be negligible.

An additional finite array calculation was performed to simulate an array in which the bursts were not simultaneous, again for an HCP array with 400m separation between bursts. In this problem, four of the outer bursts in the array were assumed to detonate 10ms early relative to the center burst, while the other two outer bursts were assumed to detonate 20ms late, as shown in Figure A.7. For this case, different edit times were used from the 2D single burst calculation to initialize the various bursts in the 3D part of the problem.

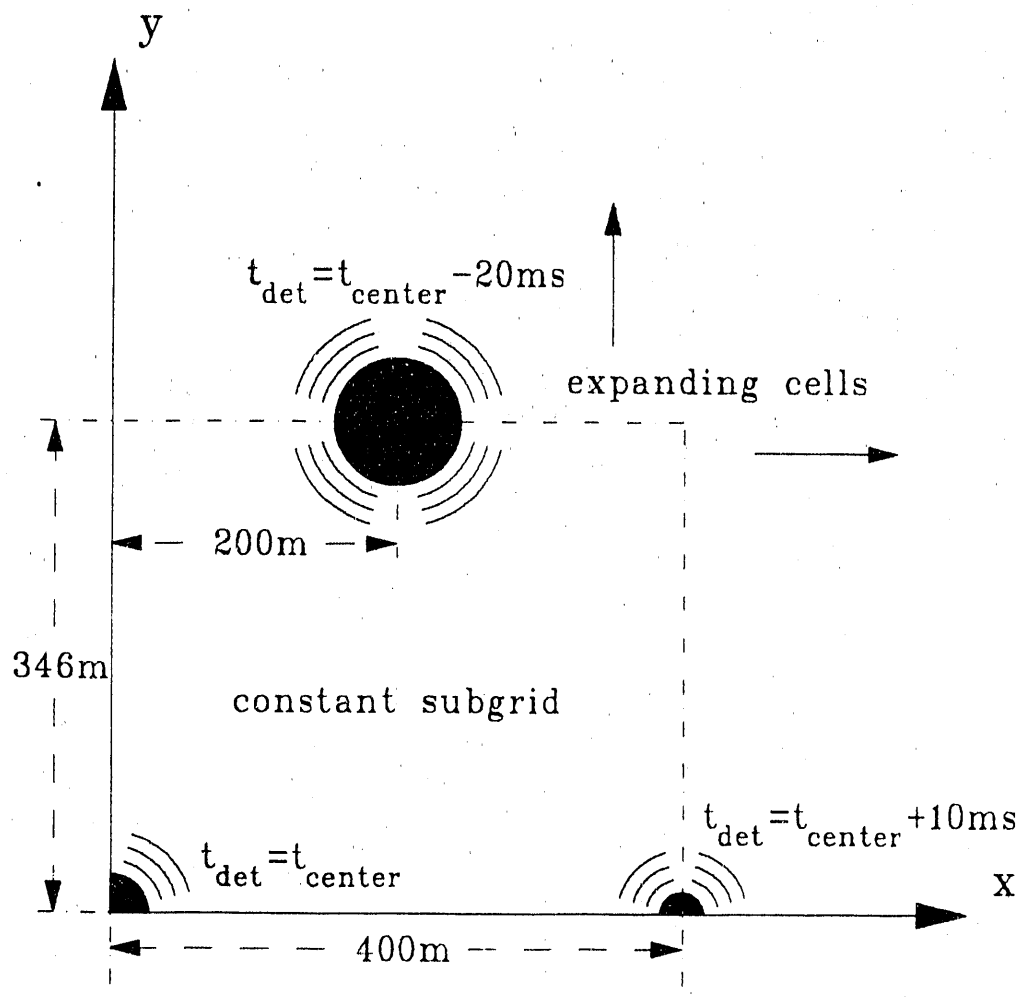

Figure A.7. Quarter-Space and Timing for Array with Non-Simultaneous Bursts

Appendix B
Results Archival

The majority of the calculations in this study were done with version 122 of the HULL [1] code, although a few of the calculations were done with version 122. A number of change decks were used to run the code on the Sandia CRAY/CTSS system and to add features required for the present studies. The change decks used for a given calculation were saved on the Sandia Integrated File Store (IFS) system, as part of the standard calculational output discussed below. The origination time and storage location for the code and change deck versions are saved in the CCL log file, for reference.

The only nonstandard change deck used for the calculations was one that implemented a special-purpose automatic rezoner. A listing of that rezoner change deck is included in the microfiche attachment.

All output files for the various calculations in this study are in the IFS directory: /e00021674/hull3-hex. Input decks can be found in the subdirectory "input-files", and sample input decks are provided also in the microfiche attachments (for a 2D single-burst calculation and for one of the 3D finite-array calculations. The other subdirectories contain:

Subdirectory	Contents
s50-hexagon	50m circular- and hexagonal-unit-cell analyses with version 120 (100m weapon spacing)
s100-hexagon	100m circular- and hexagonal-unit-cell analyses with version 120 (200m weapon spacing)
s200-hexagon	200m circular- and hexagonal-unit-cell analyses with version 120 (400m weapon spacing)
s400-hexagon	400m circular- and hexagonal-unit-cell analyses with version 120 (800m weapon spacing)
ver122-2d	200m circular-unit-cell analyses with version 122 (400m weapon spacing)
ver122-3d	200m hexagonal-unit-cell analyses with version 122 (400m weapon spacing)
200m-finite	400m-weapon-spacing finite-array analyses with version 122

The results for any given problem (depending on the set of KEEL, HULL, PULL and STATION calculations that were made) can include the following:

Filename	Description
hul4{id}{suf}{com}	binary plot/restart file
hul9{id}{suf}{com}	binary time history file

(where {id} is a one-character job identifier, {suf} is the CTSS suffix, and {com} is a nine-or-less character comment) as well as two or more of the ASCII output files:

Filename	Contents
outk{id}{suf}{com}	concatenated PLANK input/output, SAIL input/output and KEEL input/output
outck{id}{suf}{com}	change decks used in KEEL run
ship{id}{suf}{com}	concatenated PLANK input/output, SAIL input/output and HULL input
hout{id}{suf}{com}	HULL output
outch{id}{suf}{com}	change decks used in HULL run
outp{id}{suf}{com}	concatenated PLANK input/output, SAIL input/output and PULL input/output
outcp{id}{suf}{com}	change decks used in PULL run
outs{id}{suf}{com}	concatenated PLANK input/output, SAIL input/output and STATIONS input/output
outcs{id}{suf}{com}	change decks used in STATIONS run
lokh{id}{suf}{com}	CCL log file for entire run

END

DATE FILMED

10/29/90